Current Plant Biology 43 (2025) 100508

Contents lists available at ScienceDirect

Current Plant Biology

journal homepage: www.elsevier.com/locate/cpb

Sodium nitroprusside as a priming agent induces drought stress tolerance in *Citrus*

Emanuele Scialò [a], Angelo Sicilia [a,b], Angela Roberta Lo Piero [a,*]

[a] Department of Agriculture, Food and Environment, University of Catania, Catania 951213, Italy
[b] Department of Scienze Agrarie, Alimentari e Forestali, University of Palermo, Palermo 90128, Italy

ARTICLE INFO

Keywords:
Citrus
Priming
SNP
RNA-seq
WGCNA
Drought

ABSTRACT

Priming is a process whereby exposure to a mild stress or specific chemical stimulus enhances plants' resilience to future biotic and abiotic stresses. Signalling molecules such as hydrogen peroxide (H_2O_2) and nitric oxide (NO) function as priming agents. In this study, Bitters (C22) citrus rootstock was treated with the NO donor sodium nitroprusside (SNP) and subjected to drought stress. Malondialdehyde (MDA) and H_2O_2 levels were measured to assess oxidative stress. Primed plants showed significantly higher tolerance to water scarcity than non-primed ones. RNA-seq analysis revealed that priming, followed by drought stress, regulated a broad spectrum of stress responses, enhancing the expression of genes involved in photosynthetic efficiency and antioxidant activity, reallocating energy, and reinforcing external barriers and xylem vessels. As concerns phytohormones, analysis of gene expression clearly indicated that auxin biosynthesis and signalling were activated, whereas those involving ethylene were repressed. Moreover, the application of weighted gene co-expression network analysis (WGCNA) enabled the identification of genes whose expression showed positive or negative correlations with the levels of MDA and/or H_2O_2. This study provides insights into the role of priming in improving *Citrus* adaptability to water scarcity and identifying molecular strategies and candidate genes to enhance drought tolerance. To our knowledge, this is the first study correlating transcriptomic data with priming-induced drought tolerance in *Citrus*.

1. Introduction

With the global population expected to reach 9 billion by mid-century, agriculture faces the dual challenge of increasing food production while preserving environmental sustainability and ecosystem function. This challenge is further exacerbated by the ongoing effects of climate change, which hamper optimal plant growth and result in significant reductions in crop yield and biomass [1]. Drought stress, driven by limited rainfall and water availability, is a major factor causing significant and unpredictable losses in global agriculture [2,3]. This issue is expected to intensify in the near future and poses a particular challenge for *Citrus* trees, commonly grown in semi-arid regions such as southern Italy and Spain, where hot, dry summers and high evaporative demand commonly occur. Hence, both *Citrus* growth and yield and fruit quality are notably affected by water scarcity due to their high water needs [4,5].

A common strategy for enhancing drought tolerance involves using rootstocks with inherent abiotic stress resistance, a method widely adopted across various plant species [6–9], including *Citrus* spp. An appropriate rootstock can mitigate the adverse effects of environmental stresses on the scion, thereby boosting its drought resistance. By optimising the use of natural resources such as water and soil, this approach not only promotes long-term plant survival and preserves fruit quality but also reduces the use of chemical inputs [10,11].

Another approach to enhance drought tolerance involves the use of transgenes with known roles in stress resistance. For example, overexpression of the receptor-like kinase *DPY1* in foxtail millet (*Setaria italica*) improved drought tolerance by enhancing SnRK2 activation [12], as thoroughly reviewed by in [13]. Similarly, overexpression of the wheat copper chaperone gene *TaCCS1-B* and glutathione peroxidase *TaGPX1-D* in *Arabidopsis* conferred tolerance to drought and to salinity and osmotic stress, respectively [14,15]. However, this strategy relies on stable genetic transformation, which is labour-intensive, costly, time-consuming, and not widely accessible.

Priming is a process by which plants, after exposure to mild stress or chemical treatment, improve their ability to respond to future stress,

* Corresponding author.
E-mail address: rlopiero@unict.it (A.R. Lo Piero).

https://doi.org/10.1016/j.cpb.2025.100508
Received 21 March 2025; Received in revised form 4 June 2025; Accepted 7 June 2025
Available online 9 June 2025

showing enhanced resilience and biotic and abiotic stress tolerance. Upon sensing the initial stimulus, plants enter a primed state (PS), in which their defence responses towards incoming stressful conditions are activated either more rapidly, more intensely, or both. Plants can enter PS naturally due to environmental stress of different extents [16–18] or through chemical priming involving exposure to natural or synthetic priming agents [19,20]. Various molecules, such as hydrogen peroxide (H_2O_2) and nitric oxide (NO), have the potential to function as priming agents under specific conditions, enhancing plant resistance to a wide range of abiotic stresses [21]. Priming treatments do not require genetic modification. They activate the plant's endogenous stress response mechanisms, are cost-effective, and can be applied flexibly to any cultivar.

NO is a small, lipophilic, colourless diatomic gas composed of nitrogen and oxygen atoms. The ability to diffuse easily through cell membranes allows NO to function as an effective intracellular and intercellular signalling molecule in both plants and animals under normal and stress conditions [22]. In plants, NO plays a crucial role in various physiological processes, including breaking seed dormancy, promoting seed germination, root development, lateral and adventitious root formation, chlorophyll biosynthesis, vegetative growth, vascular differentiation, nodule formation, stomatal regulation, iron homeostasis, leaf senescence, flowering, and fruit ripening [23]. NO plays a crucial role in protecting plants from various environmental stresses, such as wounding, pathogen invasion, hypoxia, UV radiation, drought, salinity, temperature extremes, and heavy metal exposure [24–26]. NO is synthesized through both enzymatic and non-enzymatic pathways [27], the cytosolic nitrate reductase (NR) being a key enzymatic source under aerobic conditions [28]. The NR-dependent pathway contributes to NO production during stress responses, such as pathogen defence, drought, cold stress, stomatal regulation, iron deficiency mitigation, and root growth [29]. NO can also be generated non-enzymatically from nitrite ($NO^{2\cdot}$) in the presence of reductants like ascorbate [30]. NO is produced in various plant organelles, including chloroplasts, mitochondria, peroxisomes, cytoplasm, cell wall, and membranes [31]. The role of NO in mitigating drought stress has been demonstrated across a range of plant species, including grains, legumes, fruit trees, medicinal plants, and vegetables [32]. Due to its ability to cross biofilms and spread between cells, exogenous NO donors are commonly used to manipulate endogenous NO levels and study its regulatory mechanisms, significantly enhancing plant defence systems under abiotic stress. In soybeans, NO positively regulated the transcription of stress-adaptation-related genes, such as cytosolic glucose-6-phosphate dehydrogenase (*Cyt-G6PD)* (*GPD5*, *G6PD6*, and *G6PD7*) [33]. In drought-stressed alfalfa, over 2000 genes related to antioxidant defence, photosynthesis, hormone signalling, carbohydrate, and secondary metabolism were differentially expressed in response to NO treatment [19]. NO also induces drought-resistance genes belonging to the abscisic acid (ABA) pathway, such as *Aldehyde oxidase 3* (*AtAO3*) in *Arabidopsis thaliana*, enhancing stress tolerance [34]. Additionally, differentially expressed proteins regulated by NO donors, such as sodium hydrogen sulfide (NaHS) and sodium nitroprusside (SNP), have been identified in citrus rootstocks under polyethylene glycol (PEG)-induced drought stress through a proteomic approach [20]. In that work, it has been shown that priming could potentially enhance tolerance to subsequent drought by improving the levels of proteins involved in leaf photosynthesis, augmenting photoprotection mechanisms, and optimising photosynthetic electron transport [20]. However, the transcriptomic response to NO-induced drought tolerance in *Citrus* has not yet been investigated.

In this study, the molecular responses to SNP-induced priming followed by drought stress were investigated by analysing the transcriptome of Bitters (C22) citrus rootstock using RNA-seq and *de novo* RNA assembly approaches. Bitter (C22) was selected for this study due to its strong performance in various trials, demonstrating high yield efficiency, exceptional tolerance to calcareous soils [35], and greater resilience to PEG-induced drought stress compared to Carrizo citrange [36–38]. Additionally, the study identified the expression of genes specifically regulated by the priming treatment, suggesting their potential roles in drought resilience. Moreover, the application of weighted gene co-expression network analysis (WGCNA) coupled with gene ontology (GO) enrichment analysis performed upon the modules' eigengenes enabled the identification of categories whose expression is positively or negatively correlated with malondialdehyde (MDA) and/or H_2O_2 levels. To the best of our knowledge, this is the first report correlating transcriptomic data with priming-induced drought stress tolerance in *Citrus*.

2. Material and methods

2.1. Plant growth and experimental design

A total of 120 six-month-old Bitters (C22) plants (*C. sunki x P. trifoliata*) were evenly distributed across four pots (medium-textured sandy loam soil, 25 × 18 cm) and grown under a 16 h photoperiod (250 μmole m^{-2} s^{-1}) and 24 ± 1 °C temperature. The plants were divided into two groups and submerged in half-strength Hoagland's nutrient solution containing either distilled water or 100 μM SNP for 48 h [25,39–42]. The SNP solution was refreshed every 12 h. Following this pretreatment, all plants were left without water for 4 days. The plants were then divided into two subsets: one group received water twice a week, and the other did not in order to induce drought stress. Therefore, plants were submitted to four treatments: CK (pre-treated with distilled water without drought stress), ST (pre-treated with distilled water and then subjected to drought stress), SNP-CK (pre-treated with SNP without drought stress), and SNP-ST (pre-treated with SNP and then subjected to drought stress). Each treatment was independently run in triplicate, and each replicate consisted of ten individual plants. After thirty-four days of drought stress treatment, the leaves of each replicate were sampled, immediately frozen in liquid nitrogen and stored at −80 °C until further analyses.

2.2. Measurement of malonaldehyde and H_2O_2 content

MDA content was measured on 60 mg of leaf tissue according to the method described in López-Hidalgo *et al.* López-Hidalgo et al., [43]· H_2O_2 was determined on 50 mg of leaf tissue according to a modified version of the method described in Velikova *et al.* Velikova et al., [44].

The significance of differences for MDA and H_2O_2 measurements was tested by 2-ways ANOVA (p-value < 0.05). The statistical analyses were performed using R Studio (R version 4.4.1 (2024–06–14)) (R [45]).

2.3. Total RNA extraction

The total leaf RNA was extracted from each replicate using the RNeasy Plant Mini Kit (Qiagen, Venlo, The Netherlands) following the manufacturer's instructions. RNA degradation and contamination were monitored on 1 % agarose gels. RNA purity and concentration were checked using the NanoDrop spectrophotometer (ThermoFisher Scientific, Waltham, MA, USA). The extracted RNA from each replicate was used then for RNA-seq analysis.

2.4. Library preparation and sequencing

Before sequencing, sample RNA integrity (RIN) was assessed using the Agilent Bioanalyzer 2100 system (Agilent Technologies, Santa Clara, CA, USA), and then, sequencing libraries were generated using NEBNext® Ultra™ RNA Library Prep Kit for Illumina® (New England Biolabs, Ipswich, MA, USA) following the manufacturer's recommendations. Briefly, mRNA was enriched using poly-T oligo-attached magnetic beads. Fragmentation was carried out using divalent cations under elevated temperature in NEBNext First Strand Synthesis

Reaction Buffer (5X), followed by cDNA synthesis using random hexamers and M-MuLV Reverse Transcriptase (RNase H-). After first-strand synthesis, a custom second-strand synthesis buffer (Illumina), containing dNTPs, RNase H and Escherichia coli polymerase I, was added to generate the second strand by nick-translation. After adenylation of 3′ ends of DNA fragments, NEBNext Adaptors with hairpin loop structure were ligated to prepare for hybridisation. To select cDNA fragments preferentially 150–200 bp in length, the library fragments were purified with AMPure XP system (Beckman Coulter, Beverly, MA, USA). Then, 3 μL USER Enzyme by NEB was used with size-selected, adaptor-ligated cDNA at 37 °C for 15 min followed by 5 min at 95 °C before PCR. Successively, PCR was performed with Phusion High-Fidelity DNA polymerase, Universal PCR primers and Index (X) Primer. Library concentration was first quantified using a Qubit 2.0 fluorometer (Life Technologies, Carlsbad, CA, USA), and then diluted to 1 ng/μL before checking insert size on an Agilent Bioanalyzer 2100 system (Agilent Technologies, Santa Clara, CA, USA). Cluster generation and sequencing were performed by Novogene Bioinformatics Technology Co., Ltd. (Beijing, China). After cluster generation, the libraries were sequenced on the Illumina HiSeq2000 platform to generate pair-end reads. Raw data (raw reads) of fastq format were first processed through in-house Perl scripts. In this step, clean data were obtained by removing reads containing adapters, reads containing poly-N and low-quality reads. Then Q20, Q30, GC-content and sequence duplication level of the clean data were calculated. All the downstream analyses were based on clean, high-quality data.

2.5. *De novo transcriptome assembling and gene functional annotation*

De novo transcriptome assembly was accomplished using Trinity (2.6.6 version) with minKmerCov= 3, min_glue= 4. Then Hierarchical Clustering was performed by Corset (1.09 version) to remove redundancy (parameter -f true, Default, -m 10) and the longest transcript of each cluster was selected as Unigenes. The integrity of our assemblies was evaluated with BUSCO (Benchmarking Universal Single-Copy Orthologs), comparing Trinity.fasta, unigene.fa and cluster.fasta against the plant odb10 database to assess completeness and accuracy of splicing. Gene function was annotated based on the following databases (and software): National Centre for Biotechnology Information (NCBI) non-redundant protein sequences (Nr) and NCBI nonredundant nucleotide sequences (Nt) (NCBI blast, version 2.9.0, e-value = 1e-5), Protein family (Pfam) (hmmscan, version HMMER 3.1, parameter e-value = 0.01), Clusters of Orthologous Groups of proteins (KOG/COG) and Swiss-Prot (Diamond, version 0.8.22, parameter e-value = 1e-5), Kyoto Encyclopedia of Genes and Genomes (KEGG) (Diamond, KAAS, version 0.8.22, parameter e-value = 1e-5), and GO (blast2go, version b2g4pipe_v2.5, parameter e-value = 1e-6).

2.6. *Quantification of gene expression and differential expression analysis*

Gene expression levels were estimated by RSEM (1.2.28 version) with bowtie2 mismatch 0 parameters to map the Corset-filtered transcriptome. For each sample, clean data were mapped back onto the assembled transcriptome and read counts for each gene were obtained. Accordingly, differential expression analysis among the following comparisons was performed using the DESeq2 R package (1.26.0 version): ST vs. CK (pre-treated with distilled water and then subjected to drought stress vs. pre-treated with distilled water without drought stress), SNP-ST vs. CK (pre-treated with SNP and then subjected to drought stress vs. pre-treated with distilled water without drought stress), SNP-CK vs. CK (pre-treated with SNP without drought stress vs. pre-treated with distilled water without drought stress), SNP-ST vs. ST (pre-treated with SNP and then subjected to drought stress vs. pre-treated with distilled water and then subjected to drought stress), SNP-ST vs. SNP-CK (pre-treated with SNP and then subjected to drought stress vs. pre-treated with SNP without drought stress), and, the comparison of comparisons [(SNP-ST vs SNP-CK) vs (ST vs CK)], this last being referred to as the Priming Effect (PE) comparison specifically leading to the identification of priming-induced DEGs under drought stress condition.

The resulting p-values were adjusted using the Benjamini and Hochberg's approach for controlling the false discovery rate [46]. Genes retrieved by DESeq2 with an adjusted p-value < 0.05 were assigned as differentially expressed. A $\log_2$FoldChange threshold of ± 1 was adopted. The GO enrichment analysis of the Differentially Expressed Genes (DEGs) was implemented by ShinyGO (V0.80, corrected p-value < 0.05) [47]. Furthermore, all the unigenes were submitted to the KEGG pathway database for the systematic analysis of gene functions. KOBAS software (v3.0 version, corrected p-value < 0.05) was used to test the statistical enrichment of differentially expressed genes in KEGG pathways [48].

2.7. *Real-time validation of selected DEG candidates using RT-qPCR*

Total leaf RNA (2 μg) was reverse-transcribed using the SuperScript™ Vilo™ cDNA synthesis kit by ThermoFisher Scientific (Warrington WA1 4SR, UK). Real-time RT-qPCR was performed with PowerUp SYBR Green Master mix (ThermoFisher Scientific) and carried out in the Rotor-Gene Q (QIAGEN®, Venlo, The Netherlands). The quantification of the relative expression of a total of eight DEGs was performed in triplicate, and the fold changes were calculated by the $2^{-\Delta\Delta CT}$ method. Primers were designed using the Primer3web PCR primer design tool (version 4.1.0) and obtained by Eurofins genomics. The *Actin* housekeeping gene (NCBI: XM_006480741.4) was used as an endogenous reference. The ΔΔCT was calculated by subtracting the ΔCT of the control sample from the ΔCT of the stressed sample. The selected DEGs and their corresponding primer sequences are provided in Table S1.

2.8. *Weighted gene correlation network analysis*

Co-expression analysis was performed using the WGCNA package in R [49] to identify gene clusters with highly correlated expression profiles (hub genes). In detail, an adjacency matrix was created using FPKM values of the unigenes obtained by RNA-seq, filtered considering a threshold of FPKM > 1 in at least one sample. The pickSoftThreshold function was used to choose the proper soft-thresholding power [49]. For each analysis, the lowest power for which the scale-free topology fit index reaches 0.90 was used. The specific WGCNA analysis parameters in this study were set as follows: soft powers $\beta = 14$, WGCNA "mergeCutHeight" = 0.25. The adjacency matrix was transformed into a topological overlap matrix (TOM) as well as the corresponding dissimilarity (1-TOM). Afterwards, a hierarchical clustering dendrogram of the 1-TOM matrix was constructed to classify similar genes' expression into different gene co-expression modules. To achieve a high reliability of the results, the minimum number of genes was set to 30. The relationships between each module and either the MDA or H_2O_2 levels were estimated by calculating Pearson's correlation using the module eigengene values. Therefore, modules with high correlation coefficients and a correlation padj ≤ 0.05 were selected for subsequent analysis. Gene Significance (GS) and Module Membership (MM) were calculated, and a threshold of 0.65 was applied. Modules with correlation significance exceeding 0.7 were selected for further analysis.

3. Results

3.1. *Plant phenotype and MDA and H_2O_2 content*

After 34 days of withholding water, visual inspection showed that CK plants exhibited no signs of stress (Fig. 1A). In contrast, clear signs of water stress were observed in the ST plants (Fig. 1B), including wilting and curled yellow leaves. Similar to the CK plants, SNP-CK plants exhibited no signs of stress (Fig. 1C), while most SNP-ST plants

Fig. 1. Leaf phenotype after 34 days of drought stress. (A) CK plants, (B) ST plants, (C) SNP-CK plants, and (D) SNP-ST plants.

displayed a healthy phenotype, with only a few showing slight stress symptoms (Fig. 1D). In addition, ST plants exhibited the highest MDA values, which were significantly greater than those in the other treatments, whereas no significant differences in MDA levels were observed among the other treatments (Fig. 2A). Similarly, ST plants exhibited the highest H_2O_2 content, significantly higher than in the other treatments. CK plants had the lowest H_2O_2 levels, also significantly lower than those in the other treatments (Fig. 2B).

3.2. Transcript assembly and annotation

Raw reads were filtered to remove containing adapters reads or reads of low quality so that the downstream analyses were based on a total of 380 million clean reads with an average of ~31 million reads per sample, the average percentage of Q30 and GC being 95.34 % and 44 %, respectively (Table 1). *De novo* assembly of clean reads resulted in

Table 1
Summary statistics of the RNA quality and sequencing results.

Clean reads (million)	380
N° of transcripts	141,209
N° of Unigenes	34,516
Average of read mapping rate (%)	75.44
Transcripts N50 (bp)	2926
Unigenes N50 (bp)	2914
Q30 (%)	95.34
GC content (%)	44

141,209 transcripts and 34,516 unigenes with N50 lengths of 2926 and 2914, respectively (Table 1), indicating that good contiguity of the transcriptome has been achieved. To evaluate the assembly consistency, the filtered unique reads were mapped back to the final assembled leaf transcriptome, and the average read mapping rate using the alignment software Bowtie2 was 75.44 % (Table 1). BUSCO assessment against the 1614 gene plant odb10 set showed that our Trinity assembly recovered 1309 (81.1 %) complete orthologs (463 single-copy, 846 duplicated), with 249 (15.4 %) fragmented and only 56 (3.5 %) missing, indicating both high completeness and the expected transcript redundancy (Figure S1). Both transcripts and unigenes length distributions are reported (Figure S2). These data showed that the throughput and sequencing quality were high, allowing us to perform further analyses.

To achieve comprehensive gene functional annotation, all assembled unigenes were blasted against public databases, including the NCBI, Pfam, KOG/COG, SwissProt, Ortholog database (KO) and GO (Table 2). A total of 29,323 unigenes were annotated in at least one searched database, accounting for 84.95 % of the obtained total unigenes. Among them, 25,318 (73.35 %) and 27,458 (79.55 %) assembled unigenes showed identity with sequences in the Nr and Nt databases, respectively. The percentage of assembled unigenes homologous to sequences in KO, SwissProt, Pfam, GO and KOG databases were 26.2, 51.62, 48.43, 48.43

Table 2
The number and percentage of successfully annotated genes.

Database	Value
Annotated in Nr	25,318 (73.35 %)
Annotated in Nt	27,458 (79.55 %)
Annotated in KO	9044 (26.2 %)
Annotated in SwissProt	17,819 (51.62 %)
Annotated in Pfam	16,717 (48.43 %)
Annotated in GO	16,717 (48.43 %)
Annotated in KOG	4991 (14.45 %)
Annotated in at least one Database	29,323 (84.95 %)

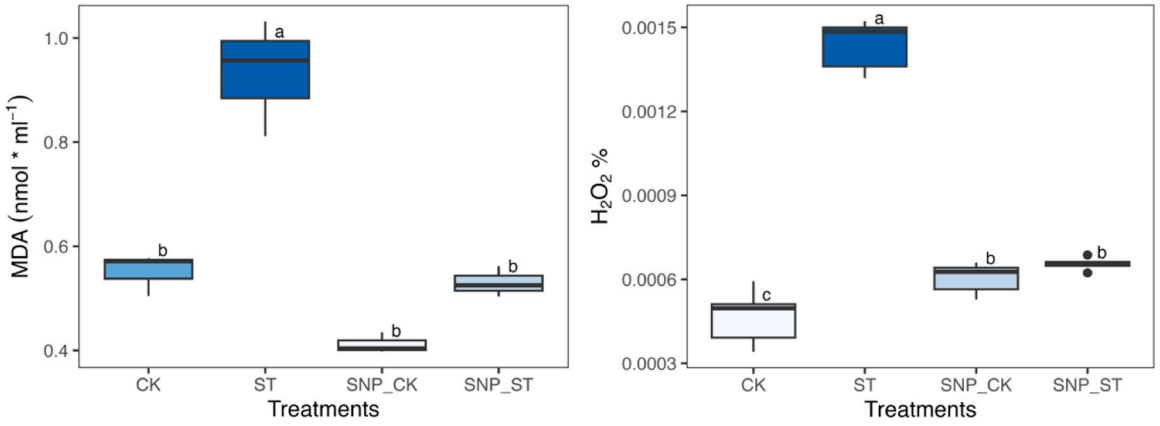

Fig. 2. Box plot of the malondialdehyde (MDA) (A) and hydrogen peroxide (H_2O_2) (B) content in control (CK), stressed (ST), pre-treated control (SNP-CK), and pre-treated stressed (SNP-ST) plants after 34 days of drought stress. Lower and upper box boundaries 25th and 75th percentiles, respectively, line inside box median, lower and upper error lines 10th and 90th percentiles, respectively, filled circles data falling outside 10th and 90th percentiles. Different letters indicate significantly different values ($p < 0.05$).

and 14.45 %, respectively (Table 2).

The PCA of normalised gene expression data from CK, ST, SNP-CK, and SNP-ST samples revealed tight clustering of the three biological replicates within each treatment, indicating strong consistency across replicates. Notably, the control groups (CK and SNP-CK) clustered closely together, suggesting minimal or no significant differences in their transcriptomes. In contrast, the ST plants formed a distinct cluster, far removed from the control groups, reflecting substantial transcriptional changes induced by drought stress. Interestingly, SNP-ST plants positioned themselves between the control and ST clusters, indicating that SNP priming modulated the transcriptomic response to drought, resulting in an intermediate expression profile between stressed and non-stressed plants (Figure S3).

3.3. Identification of Differentially Expressed Genes (DEGs)

The characterisation of the citrus plant's transcriptional response to the SNP-priming pre-treatment followed by drought stress was carried out by the identification of the unigenes whose expression level changed upon different treatments. A total of 41 DEGs (8 upregulated and 33 downregulated genes) were identified in the SNP-CK vs CK comparison, 3489 DEGs (1168 upregulated and 2321 downregulated genes) in the SNP-ST vs CK comparison, 3556 DEGs (1319 upregulated and 2237 downregulated genes) in the SNP-ST vs SNP-CK comparison, 5122 DEGs (2566 upregulated and 2556 downregulated genes) in the SNP-ST vs ST comparison, and 9393 DEGs (4402 upregulated and 4991 downregulated genes) in the ST vs CK comparison. A total of 4369 DEGs (2629 upregulated and 1740 downregulated) were identified in the Priming Effect (PE) comparison, specifically leading to the identification of priming-induced DEGs under drought stress conditions (Fig. 3).

The validation of expression levels for eight selected DEG candidates was carried out by quantitative real-time PCR (RT-qPCR). The results show high congruence between RNA-seq results and RT-qPCR analysis (coefficient of determination $R^2 = 0.91$), indicating the reliability of RNA-seq in the quantification of gene expression (Figure S4).

3.4. Functional classification of DEGs

GO terms and KEGG pathway functional enrichment analyses of DEGs were conducted to identify key biological processes and pathways involved in the plant's response to SNP-induced priming.

3.4.1. GO enrichment analysis

To gain a clearer understanding of the effects of the sole SNP priming treatment on the plant, we conducted an enrichment analysis on the SNP-CK vs CK comparison, as shown in Fig. 4. Despite the relatively low number of DEGs (41), the SNP-CK vs CK comparison revealed significant enrichment in several functional terms. Remarkably, all the enriched terms were associated with processes related to cell wall biogenesis and polysaccharide metabolism, suggesting that the priming treatment specifically influenced cell wall regulation under normal watering conditions.

Given that the SNP priming treatment had minimal impact on the plant, as evidenced by the extremely low number of DEGs in the SNP-CK vs CK comparison and the enrichment of GO terms exclusively related to cell wall metabolism, further analyses were conducted on the set of DEGs identified in the PE comparison to evaluate the effect of SNP priming under drought stress conditions.

The PE comparison revealed enrichment for 20 terms within the Molecular Function category (Fig. 5A). Notably, the most enriched term was "Methyl indole-3-acetate esterase activity", which plays a role in auxin-mediated signalling pathways. Other significantly enriched terms were related to various signalling pathways, including "Transmembrane signalling receptor activity", "Transmembrane receptor protein kinase activity", "Signalling receptor activity", and "Molecular transducer activity". These terms highlight the involvement of complex receptor-mediated signalling mechanisms that likely contribute to the plant's regulation of stress responses and cellular communication under drought conditions.

The PE comparison also revealed enrichment for 19 terms within the Biological Process category (Fig. 5B). The most prominently enriched term was "Photosynthetic electron transport in Photosystem I". Notably,

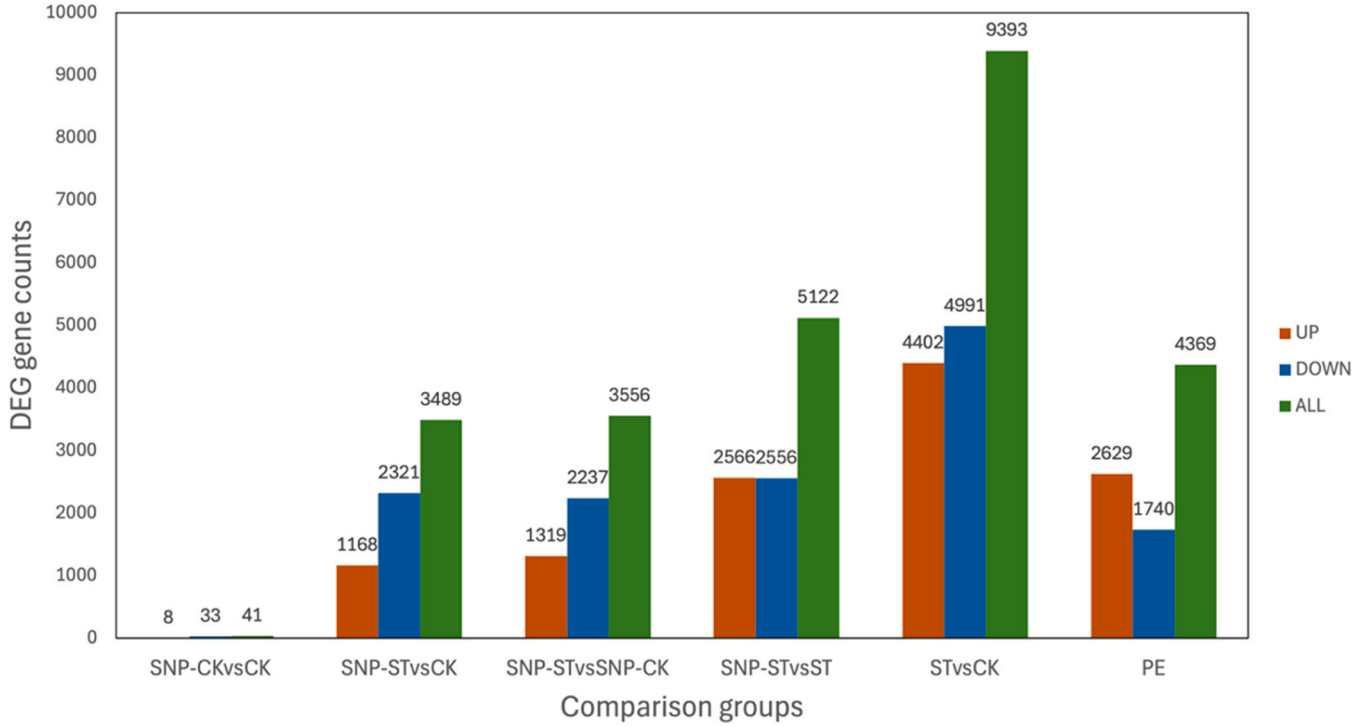

Fig. 3. Bar plot showing the differentially expressed genes (DEGs) in the SNP-CK vs. CK, SNP-ST vs. CK, SNP-ST vs. SNP-CK, SNP-ST vs. ST, ST vs. CK, and PE comparisons adopting a $\log_2$FoldChange threshold of 1 (2.0 fold change).

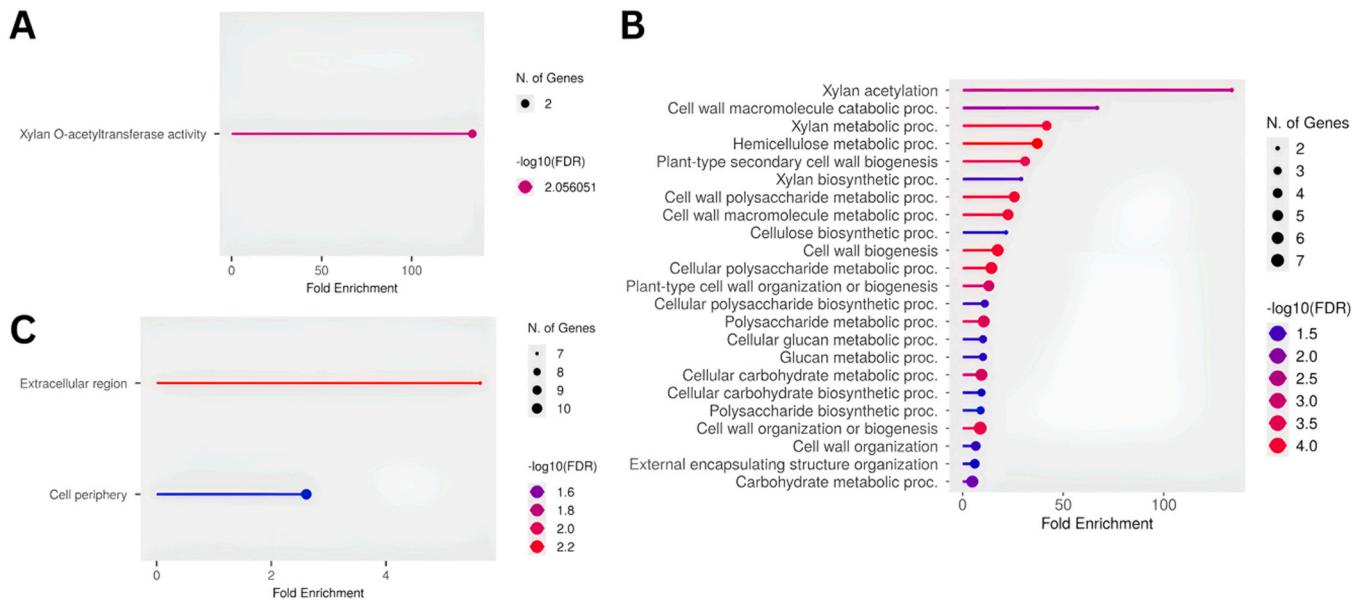

Fig. 4. Lollipop plot showing the Gene Ontology (GO) enrichment analysis for the DEGs in the SNP-CK vs CK comparison. (A) Molecular Function, (B) Biological Process, and (C) Cellular Component categories. The X-axis represents the Fold Enrichment, while the Y-axis lists the enriched GO terms. The colour gradient of the dots represents the -log10(FDR), with darker colours indicating higher statistical significance (lower FDR values). The size of the dots corresponds to the number of genes associated with each GO term.

several other photosynthesis-related terms were also enriched, including “Photosynthesis”, “Photosynthetic electron transport chain”, and “Photosynthesis light reaction”, underscoring the importance of photosynthetic processes in the investigated conditions. Additionally, several terms related to cell wall metabolism were significantly enriched, such as “Cell wall organization”, “Cell wall organization or biogenesis”, “Plant-type secondary cell wall biogenesis”, “Phloem or xylem histogenesis”, and “Xylem development”. These findings suggest a focus on structural and developmental changes in the plant’s cell wall and vascular tissues. The enrichment of the term "Regulation of hormone levels" points to the involvement of hormone signalling pathways, indicating their role in regulating the plant’s response to stress and development.

Lastly, the analysis revealed enrichment for 11 terms within the Cellular Component category (Fig. 5C). The most enriched term was “Photosystem I”, a crucial component in the photosynthetic machinery, followed by “Photosystem”, highlighting the impact on photosynthetic structures. Additionally, several terms related to the cell periphery were significantly enriched, including “Anchored component of membrane”, “Anchored component of plasma membrane”, “Intrinsic component of plasma membrane”, “Plasma membrane”, “Cell periphery”, “Apoplast”, and “Cell wall”. These terms emphasise the role of membrane-associated and structural components in the cellular response to the experimental conditions.

3.4.2. KEGG enrichment analysis

Fig. 6 presents the main KEGG pathways, ranked by decreasing significance (adjusted p-value). The PE comparison revealed significant enrichment for 14 pathways. Among these, the most enriched were “Metabolic pathways” and “Biosynthesis of secondary metabolites”. Pathways involved in energy production and carbon flow were also significantly enriched, including “Carbon metabolism”, “Glyoxylate and dicarboxylate metabolism”, “Carbon fixation in photosynthetic organisms”, and “Galactose metabolism”. In terms of secondary metabolism, pathways such as “Isoquinoline alkaloid biosynthesis”, “Phenylalanine metabolism”, and “Tyrosine metabolism” showed strong enrichment, highlighting their involvement in specialised compound production. Additionally, pathways related to photosynthesis and carbon storage, such as “Photosynthesis” and “Starch and sucrose metabolism”, were enriched, indicating their critical roles in energy conversion and storage under stress conditions. Notably, the “ABC transporters” category, which is responsible for transporting various molecules across cellular membranes, had the highest gene ratio among the significantly enriched terms, suggesting a crucial involvement of cellular transport processes during the experiment.

3.5. Analysis of transcription factor gene families

The sets of DEGs encoding transcription factors (TFs) were identified and categorised into families for the PE comparison. Fig. 7 presents the number of both upregulated and downregulated DEGs across the ten most abundant TF families, ranked by the total number of genes. The identified DEGs include 28 belonging to the NAC family, 21 to MYB, 21 to AP2/ERF-ERF, 14 to Others, 13 to GRAS, 13 to WRKY, 12 to bHLH, 12 to MYB-related, 11 to AUX/IAA, and 9 to C2H2 families. Notably, the analysis revealed that most of the families exhibited substantially more upregulated genes than downregulated genes. However, AP2/ERF-ERF and WRKY represented the exceptions, showing a higher number of downregulated genes. This analysis highlights the TF families whose gene expression was most affected by the experimental conditions, particularly the prominent upregulation in response to SNP-induced priming to cope with drought stress.

3.6. Identification of functional genes related to drought stress tolerance

To unravel *Citrus* responses to SNP-priming under drought, we analysed the list of DEGs belonging to the most enriched GO terms (Fig. 5) and KEGG pathways (Fig. 6) from the PE comparison, focusing on genes known to be related to water scarcity from drought sensing and signalling to the main downstream metabolisms [50,51].

3.6.1. Drought sensing and signalling

As shown in Table 3, the analysis of DEGs related to drought sensing and signalling revealed the upregulation of *C. sinensis* receptor-like protein kinase FERONIA and homolog to *A. thaliana* receptor-like protein kinase THESEUS1. These receptor-like kinases are essential for cell wall remodelling and integrity sensing, primarily acting in a brassinosteroid (BR)-independent manner [52–54]. Additionally, *C. sinensis*

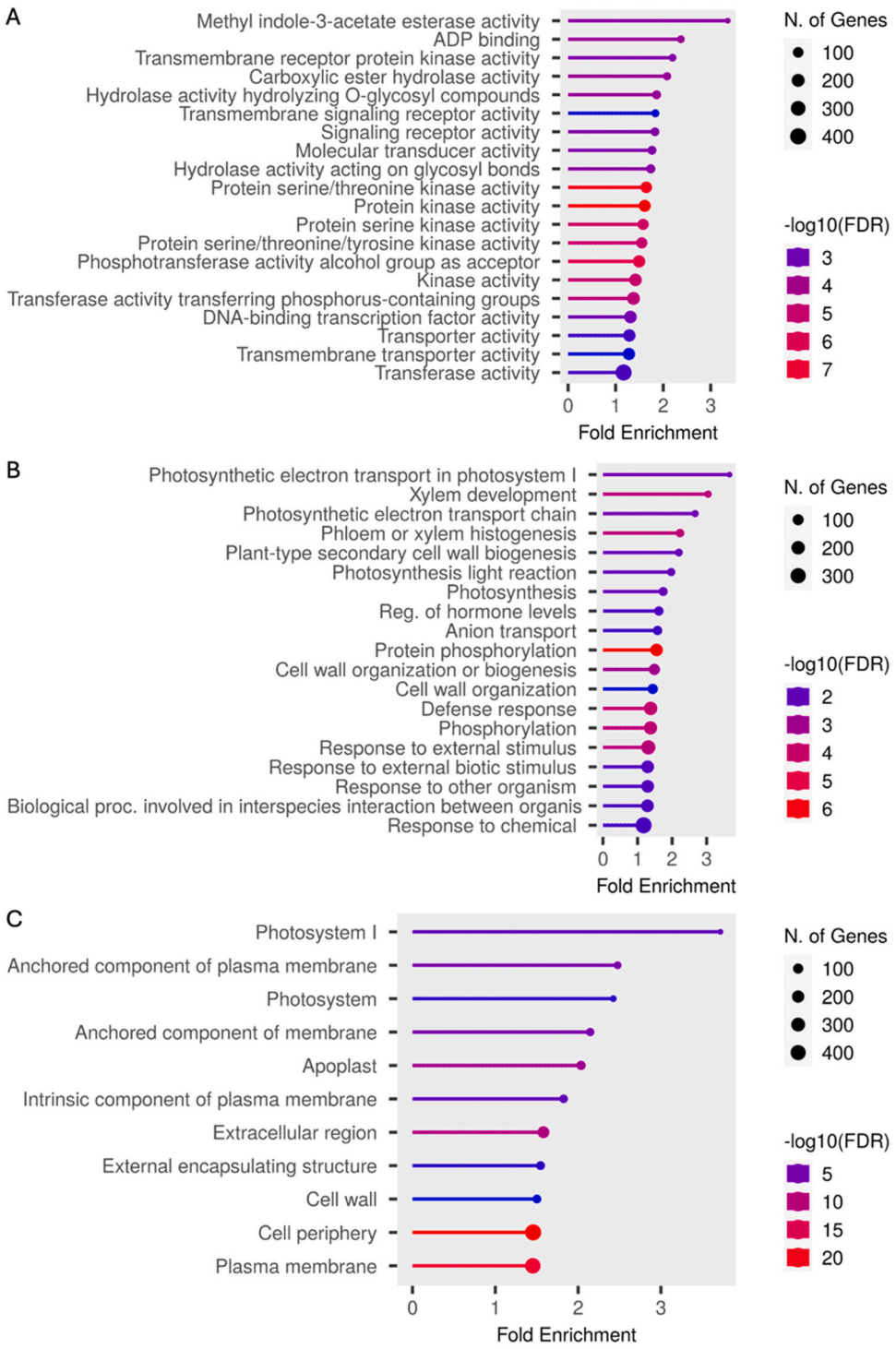

Fig. 5. Lollipop plot showing the Gene Ontology (GO) enrichment analysis for the DEGs in the PE comparison. (A) Molecular Function, (B) Biological Process, and (C) Cellular Component categories. The X-axis represents the Fold Enrichment, while the Y-axis lists the enriched GO terms. The colour gradient of the dots represents the -log10(FDR), with darker colours indicating higher statistical significance (lower FDR values). The size of the dots corresponds to the number of genes associated with each GO term.

wall-associated receptor kinase 2-like (WAK2-like), also involved in cell expansion and development [55], was found to be upregulated. Homolog to *A. thaliana* Cold-responsive protein kinase 1 (CRPK1), a negative regulator of freezing tolerance [56], was found to be upregulated. *C. sinensis* mechanosensitive ion channel protein 10-like (MSL10), a mechanosensitive channel that transduces mechanical force into ion flux, providing a mechanism for the perception of mechanical stimuli such as sound, touch and osmotic pressure [57], was found to be upregulated. Similarly, *C. sinensis* MID1-complementing activity 1 (MCA1), a mechanosensitive channel proposed to mediate the perception of hydraulic pressure changes under dehydration stress [58] and to enhance cold tolerance in *Arabidopsis* [59], was found to be upregulated. *C. sinensis* leucine-rich repeat receptor protein kinase HPCA1 was found to be upregulated. HPCA1 is activated by H_2O_2 and mediates H_2O_2-induced activation of Ca^{2+} channels in guard cells, playing a crucial role in stomatal closure [60]. On the other hand, *C. sinensis* E3 ubiquitin-protein

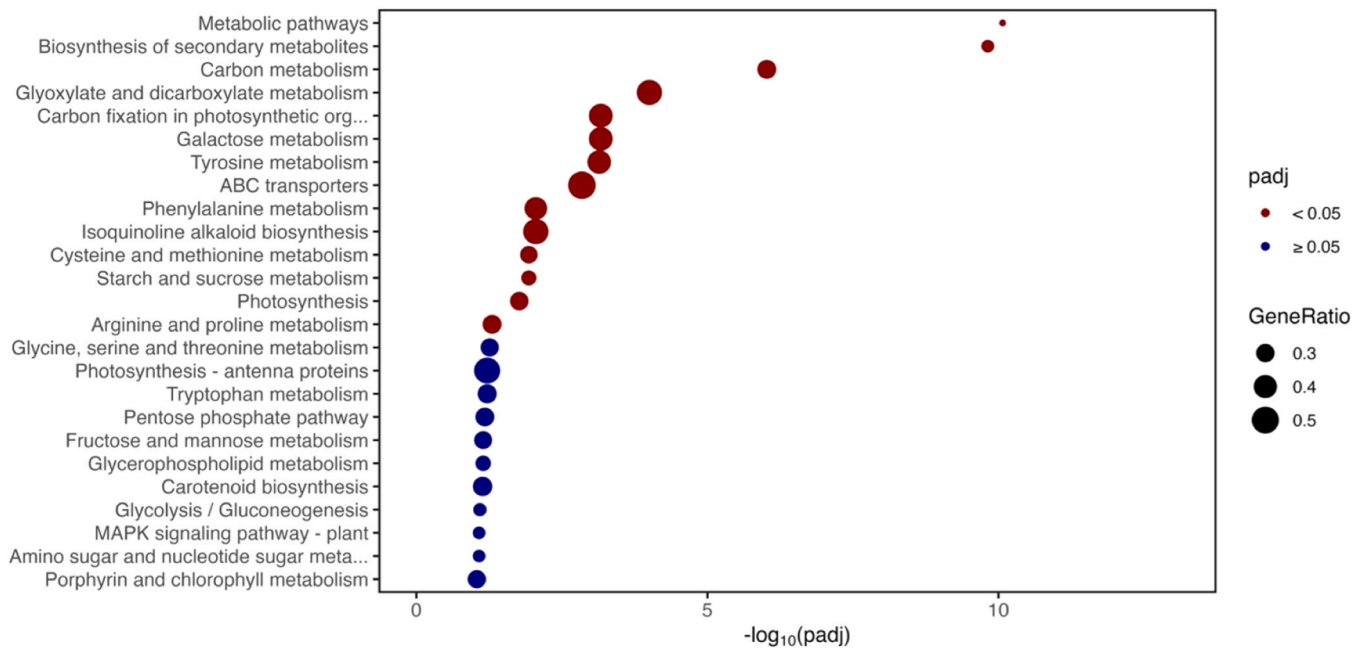

Fig. 6. Dot plot of the Kyoto Encyclopaedia of Genes and Genomes (KEGG) enrichment analysis for the PE comparison. The X-axis represents the -log10(padj). The Y-axis lists the enriched KEGG pathways. The colour of each dot indicates the level of statistical significance: red for pathways with a padj < 0.05, and blue for pathways with a padj ≥ 0.05. The size of the dots corresponds to the gene ratio.

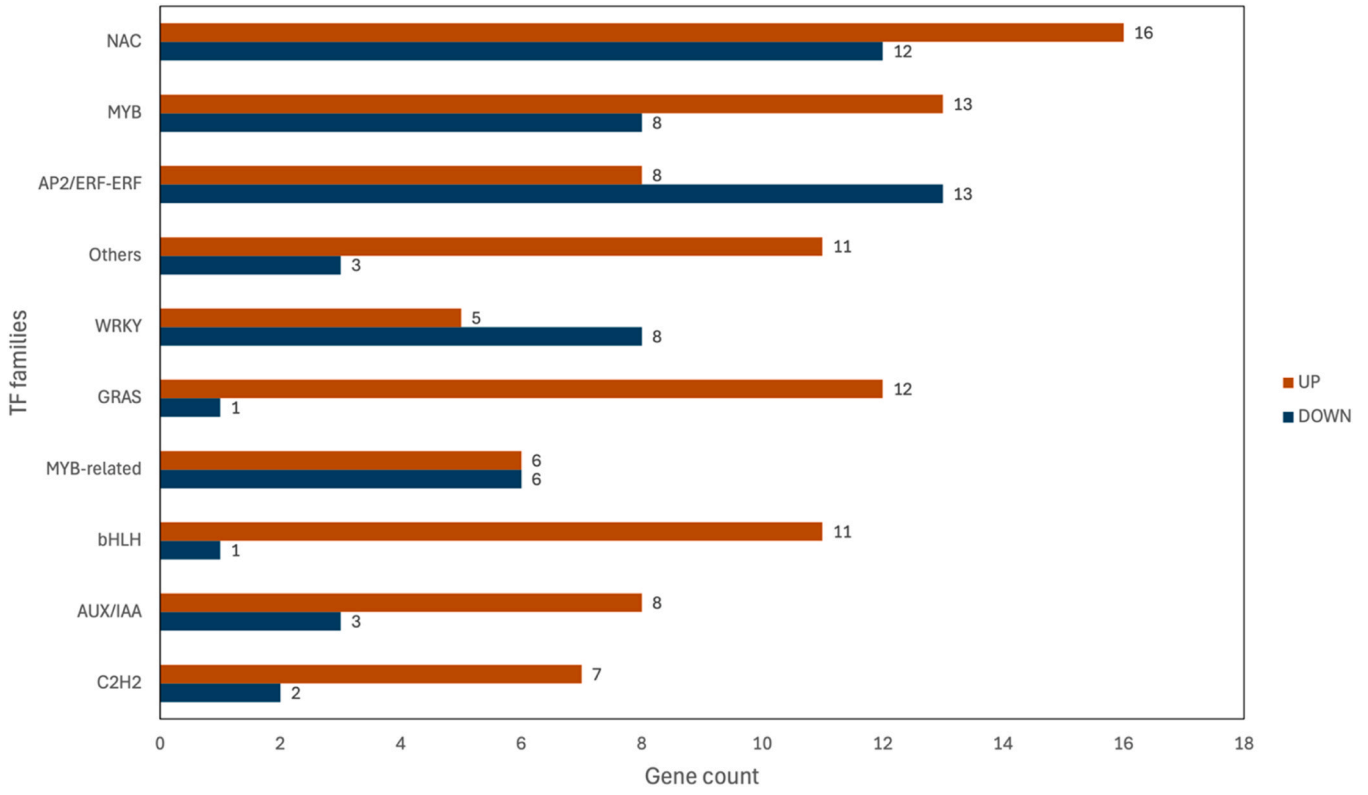

Fig. 7. Bar plot showing the distribution of the ten most abundant families of transcription factors responsive to SNP-induced priming to control drought stress in the PE comparison. The X-axis represents the number of genes that are either upregulated (depicted in red) or downregulated (depicted in blue) for each TF family. The Y-axis lists the names of the transcription factor families.

ligases PUB24-like and PUB23-like were downregulated. These genes are known negative regulators of PTI (pattern-triggered immunity) in response to various PAMPs (pathogen-associated molecular patterns) [61]. Additionally, PUB23 also plays a role as a negative regulator in the water stress response [62]. Furthermore, the *C. sinensis* L-type lectin-domain containing receptor kinase IX.1-like, which is associated with *Phytophthora* resistance, H_2O_2 production, and cell death [63], and *C. sinensis* bidirectional sugar transporter SWEET15, which mediates

Table 3
List of DEGs related to drought stress signalling identified in PE comparison.

Cluster ID	Database description	Evalue	log_2 fold change
Drought sensory and signalling mechanisms			
3427.20522	*A. thaliana* Receptor-like protein kinase THESEUS 1 (Q9LK35)	0	+ 3.8
3427.21706	*Citrus sinensis* wall-associated receptor kinase 2-like (WAK2-like) (LOC127899629)	0	+ 3.6
3427.4092	*A. thaliana* Cold-responsive protein kinase 1 (CRPK1) (Q93YN1)	3.92E−71	+ 3.6
3427.8717	*Citrus sinensis* mechanosensitive ion channel protein 10-like (MSL10) (LOC102625242)	0	+ 3.3
3427.19304	*Citrus sinensis* leucine-rich repeat receptor protein kinase HPCA1 (LOC102619900)	0	+ 3.3
3427.15341	*Citrus sinensis* receptor-like protein kinase FERONIA (LOC102609835)	0	+ 2.4
3427.9390	*Citrus sinensis* MID1-COMPLEMENTING ACTIVITY 1 (MCA1) (LOC102609339)	0	+ 2.1
3427.27077	*Citrus sinensis* E3 ubiquitin-protein ligase PUB24-like (LOC102626705)	0	−6.9
3427.3177	*Citrus sinensis* E3 ubiquitin-protein ligase PUB23-like (LOC102631041)	0	−3.8
3427.25668	*Citrus sinensis* L-type lectin-domain containing receptor kinase IX.1-like (LOC102626532)	0	−3.8
3427.11041	*Citrus sinensis* bidirectional sugar transporter SWEET15 (LOC102611503)	0	−2.6

both low-affinity uptake and efflux of sugar across the plasma membrane, were also downregulated (Table 3).

3.6.2. Hormone regulation

The analysis of DEGs related to plant hormone regulation revealed DEGs associated with ethylene, auxin, abscisic acid (ABA), and gibberellic (GA) signalling (Table 4).

3.6.2.1. Ethylene. *C. clementina* 1-aminocyclopropane-1-carboxylate synthase 1 (ACS1), which catalyses the formation of 1-aminocyclopropane-1-carboxylate (ACC), a key precursor in ethylene biosynthesis in higher plants, was found to be strongly downregulated. Additionally, *C. clementina* 1-aminocyclopropane-1-carboxylate oxidase (ACO), responsible for the final step in ethylene production in plant tissues, also exhibited down-regulation. *C. clementina* ethylene receptor 2 (ETR2), part of the ETR family, which negatively regulates ethylene response pathways in the absence of ethylene [64], was also found to be downregulated (Table 4).

3.6.2.2. Auxin. *C. sinensis* probable N-acetyltransferase HLS1, which plays a negative role in sugar and auxin signalling, and the negative feedback regulation of free IAA level [65] was upregulated. Similarly, *C. clementina* protein kinase PINOID (PID), which encodes a serine-threonine protein kinase, was upregulated. It has been shown that PINOID functions as a positive regulator of polar auxin transport and that it is involved in the fine-tuning of polar auxin transport during organ formation in response to local auxin concentrations [66,67]. Also, the PINOID-dependent binary switch controls PIN polarity and mediates changes in auxin flow to create local gradients for patterning processes [68]. Interestingly, *C. sinensis* auxin efflux carrier component 6 (PIN6), involved in the regulation of auxin homeostasis during plant development [69], and *C. sinensis* choline transporter protein 1 (CHER1), involved in the regulation of intracellular trafficking of PIN-type auxin transporters [70], were also upregulated. *C. sinensis* methylesterase 17-like, a methylesterase that efficiently and specifically hydrolyses methyl indole-3-acetic acid (MeIAA), the inactive form of IAA, into the active auxin (IAA) [71], was upregulated. *C. sinensis* serine/threonine-protein kinase D6PK, a protein kinase that regulates the auxin transport activity of PIN auxin efflux facilitators and promotes auxin transport in the hypocotyl [72,73]. Similarly, *C. clementina* receptor-like kinase TMK4, involved in auxin signal transduction, cell expansion and proliferation regulation [74], as well as *C. sinensis* protein BIG GRAIN 1-like B and E, regulators of the auxin signalling pathway were upregulated (Table 4).

Table 4
List of DEGs related to hormone regulation of drought stress response identified in PE comparison.

Cluster ID	Database description	Evalue	log_2 fold change
Hormone regulation of drought stress response			
Ethylene			
3427.1691	*Citrus clementina* 1-aminocyclopropane−1-carboxylate synthase 1 (ACS1) (LOC18048242)	0	−12.6
3427.10612	*Citrus clementina* 1-aminocyclopropane−1-carboxylate oxidase (ACO) (LOC18050524)	0	−2.4
3427.7602	*Citrus clementina* ethylene receptor 2 (ETR2) (LOC18031847)	0	−3
Auxin			
3427.2815	*Citrus sinensis* auxin efflux carrier component 6 (PIN6) (LOC102617173)	0	+ 5.5
3427.7124	*Citrus sinensis* N-acetyltransferase HLS1 (LOC102630697)	0	+ 4.8
3427.4154	*Citrus clementina* protein kinase PINOID (LOC18052602)	0	+ 3.5
3427.9750	*Citrus sinensis* methylesterase 17-like (MES17) (LOC102625455)	0	+ 2.3
3427.8153	*Citrus sinensis* serine/threonine-protein kinase D6PK (LOC102626820)	0	+ 2.3
3427.19486	*Citrus clementina* receptor-like kinase TMK4 (LOC18031913)	0	+ 2.3
3427.6410	*Citrus sinensis* BIG GRAIN 1-like B (LOC102611186)	0	+ 2.3
3427.23175	*Citrus sinensis* BIG GRAIN 1-like E (LOC102619821)	0	+ 2.1
3427.10772	*Citrus sinensis* choline transporter protein 1 (CHER1) (LOC102619733)	0	+ 2.1
ABA			
3427.27931	*Citrus clementina* arm repeat protein interacting with ABF2 (ARIA) (LOC18046112)	0	+ 5.3
3427.2423	*Citrus sinensis* E3 ubiquitin-protein ligase RHA2A (LOC107174311)	0	+ 4.6
3427.26261	*Citrus clementina* E3 ubiquitin-protein ligase KEG (LOC18040779)	0	−2.5
Gibberellin			
3427.29625	*Citrus sinensis* gibberellic acid methyltransferase 2 (GAMT2) (LOC102631417)	0	+ 3.3
3427.609	*Citrus sinensis* DELLA protein RGL1-like (LOC102621825)	0	+ 3.2

3.6.2.3. ABA. In the PE comparison, only a few genes directly involved in ABA signalling and drought responses were found to be deregulated. *C. clementina* ARM REPEAT PROTEIN INTERACTING WITH ABF2 (ARIA), which acts as a positive regulator of ABA response via the modulation of the transcriptional activity of ABF2 [75], was found upregulated. *C. sinensis* E3 ubiquitin-protein ligase RHA2A, which plays a role in the positive regulation of ABA signalling and responses to salt, osmotic stress [76], and drought [77], was upregulated. Concordantly, *C. clementina* E3 ubiquitin-protein ligase KEG, a negative regulator of abscisic acid signalling [78], was found to be downregulated (Table 4).

3.6.2.4. GA. Similarly to ABA, in the PE comparison, only two genes directly involved in gibberellin (GA) regulation were deregulated. *C. sinensis* gibberellic acid methyltransferase 2 (GAMT2), which methylates the carboxyl group of various gibberellins to deactivate them and initiate their degradation [79], and *C. sinensis* DELLA protein RGL1-like,

which acts as a repressor of the GA signalling [80], were found to be upregulated (Table 4).

3.6.3. Transcription factors

The analysis of the ten most abundant TF families among the list of DEGs within the PE comparison allowed the identification of genes that might play a role in the SNP-induced tolerance to drought stress (Table 5).

3.6.3.1. AP2/ERF. Ten ethylene-responsive transcription factors were found to be differentially expressed, with four upregulated and six downregulated. Among these, *C. clementina* ethylene-responsive transcription factor 1B (ERF1B), a key regulator involved in integrating ethylene and jasmonate signals to modulate defence response genes [81, 82], was downregulated. ERF1 has been shown to confer resistance against necrotrophic fungi such as *B. cinerea* and *Plectosphaerella cucumerina*, though its overexpression in *Arabidopsis* reduces tolerance to *Pseudomonas syringae* tomato DC3000, indicating negative crosstalk between ethylene and salicylic acid signalling pathways [83]. Additionally, *C. sinensis* dehydration-responsive element-binding protein 3 (DREB3), known to be upregulated in response to drought stress in citrus [37], was found to be upregulated. In contrast, *C. sinensis* dehydration-responsive element-binding protein 2A (DREB2A), which is involved in heat stress-inducible gene expression [84], was downregulated (Table 5).

3.6.3.2. Other. *C. clementina* GATA transcription factor 4 (GATA4), involved in regulating light-responsive genes [85], was upregulated. Additionally, a homolog to *A. thaliana* calmodulin-binding transcription activator 4 (CAMTA4), which plays a role in the positive regulation of the general stress response (GSR) via Ca^{2+} signalling [86], was also upregulated. Furthermore, *C. clementina* homeobox-leucine zipper protein HDG11, a positive regulator of drought stress tolerance that can transactivate several cell-wall-loosening protein genes [87], was found to be upregulated (Table 5).

3.6.3.3. WRKY. Several WRKY transcription factors were deregulated in the PE comparison, with the majority showing down-regulation. These transcription factors are known to play a crucial role in basal defence mechanisms. Notably, *C. sinensis* WRKY transcription factor 72A-like, the most downregulated gene, is known to contribute to basal defence against root-knot nematodes (RKNs) and potato aphids [88]. Additionally, it is involved in the transcriptional regulation of terpene biosynthesis [89] (Table 5).

3.6.3.4. NAC. *C. sinensis* NAC domain-containing protein 76-like (NAC076), which promotes xylem formation by enhancing the expression of secondary wall-associated genes [90], and NAC domain-containing protein 12-like (NAC012), required for the secondary cell wall thickening and lignification of sclerenchymatous fibres and secondary xylem vessels, were upregulated in SNP-primed plant in drought conditions (Table 5).

3.6.3.5. MYB. *C. sinensis* transcription factor MYB61 was found to be upregulated. This transcription factor coordinates a small network of downstream target genes essential for various aspects of plant growth and development, including xylem formation and xylem cell differentiation [91]. Additionally, MYB61 plays a role in regulating stomatal pore size independently of ABA [91]. Similarly, *C. sinensis* MYB124, homolog to *A. thaliana* MYB88, which ensures that stomata contain just two guard cells (GCs) by enforcing a single symmetric precursor cell division before stomatal maturity [92], was found upregulated. Furthermore, *C. sinensis* transcription factor MYB16, which functions as a major regulator of cuticle formation in vegetative organs by regulating cuticle biosynthesis genes [93], was also found upregulated (Table 5).

Table 5
List of DEGs related to DNA binding activity during drought stress response identified in PE comparison.

Cluster ID	Database description	Evalue	log_2 fold change
Transcription factors			
Other			
3427.760	*Citrus clementina* GATA transcription factor 4 (GATA4) (LOC18047164)	0	+ 2.3
3427.28689	*Citrus clementina* homeobox-leucine zipper protein HDG11 (LOC18050300)	0	+ 2.1
3427.7521	*A. thaliana* Calmodulin-binding transcription activator 4 (CAMTA4) (Q9FYG2)	5.09E−40	+ 2.1
WRKY			
3427.1511	*Citrus sinensis* WRKY transcription factor 72A-like (LOC102628632)	0	−5.6
3427.4282	*Citrus sinensis* WRKY transcription factor 28-like (LOC102629968)	0	−3.9
3427.1430	*Citrus sinensis* WRKY transcription factor 14 (LOC102627217)	0	−3.5
3427.23231	*Citrus sinensis* WRKY transcription factor 75 (LOC102622530)	0	−2.7
3427.6170	*Citrus sinensis* WRKY transcription factor 23 (LOC102612245)	0	−2.2
NAC			
3427.29040	*Citrus sinensis* NAC domain-containing protein 12-like (LOC102629852)	0	+ 4.8
3427.29448	*Citrus sinensis* NAC domain-containing protein 76-like (LOC102610635)	0	+ 3.1
MYB			
3427.5984	*Citrus sinensis* transcription factor MYB61 (LOC102609163)	0	+ 4
3427.4409	*Citrus sinensis* transcription factor MYB16 (LOC102621582)	0	+ 3.6
3427.8361	*Citrus sinensis* transcription factor MYB124 (LOC102629689)	0	+ 1.9
3427.26084	*Citrus sinensis* transcription factor MYB73-like (LOC102624059)	0	−2.2
AP2/ERF			
3427.29139	*Citrus clementina* ethylene-responsive transcription factor 13 (LOC18047940)	0	+ 5
3427.7818	*Citrus sinensis* ethylene-responsive transcription factor ERF038 (LOC102620560)	0	+ 3.5
3427.3222	*Citrus sinensis* ethylene-responsive transcription factor ERF039 (LOC102611994)	0	+ 2.7
3427.18626	*Citrus sinensis* ethylene-responsive transcription factor 13 (LOC102629320)	0	+ 2.2
3427.8521	*Citrus sinensis* dehydration-responsive element-binding protein 3 (DREB3) (KAH9714206)	0	+ 1.5
3427.26945	*Citrus clementina* ethylene-responsive transcription factor ERF096 (LOC18033206)	0	−8.7
3427.12120	*Citrus sinensis* ethylene-responsive transcription factor ERF110 (LOC102622241)	0	−5.4
3427.30403	*Citrus sinensis* ethylene-responsive transcription factor ERN1 (LOC102618007)	0	−3.5
3427.7677	*Citrus clementina* ethylene-responsive transcription factor 1B (LOC18046781)	0	−2.5
3427.7616	*Citrus sinensis* dehydration-responsive element-binding protein 2 A (DREB2A) (LOC102610198)	0	−1.4
GRASS			
3427.9505	*Citrus clementina* SCARECROW-LIKE protein 7 (SCL7) (LOC18037057)	0	+ 2.1
3427.5941	*Citrus sinensis* protein SHORT-ROOT-like (LOC102610900)	0	+ 2

3.6.3.6. GRASS. C. clementina SCARECROW-LIKE protein 7 (SCL7), which is involved in conferring resistance to environmental abiotic stresses, particularly salt and drought, by enhancing the expression of stress-responsive genes [94], was upregulated. Similarly, *C. sinensis* SHORT-ROOT-like protein, a general regulator of cell proliferation in leaves [95] and essential for bundle sheath cell fate specification [96], p. 2, was upregulated. Interestingly, these functions are also regulated by the Scarecrow gene family [96], p. 2; [95]; Table 5.

3.6.4. Photosynthesis

Among the deregulated genes involved in the photosynthetic process, several clusters associated with photosystems I and II were found to be upregulated. Interestingly, *C. sinensis* ATP-dependent zinc metalloprotease FTSH 6, a chloroplastic-like protein involved in the degradation of the light-harvesting complex of photosystem II (LHC II) [97], was observed to be downregulated. Furthermore, *C. sinensis* beta carbonic anhydrase 1 (BCA1), involved in the CO_2 signalling pathway which controls gas exchange between plants and the atmosphere by modulating stomatal development and movements [98], was found to be upregulated (Table 6).

3.6.5. Carbon metabolism

Several genes associated with the pentose phosphate pathway (PPP) and the Calvin cycle were found to be downregulated (Table 6).

Table 6
List of DEGs related to drought stress response identified in PE comparison.

Cluster ID	Database description	Evalue	log_2 fold change
Photosynthesis			
3427.14244	*Citrus clementina* photosystem I subunit O (LOC18035077)	0	+ 2.5
3427.15315	*Citrus sinensis* beta carbonic anhydrase 1 (BCA1)	0	+ 2.5
3427.14552	*Citrus clementina* oxygen-evolving enhancer protein 3, chloroplastic (LOC18051773)	0	+ 2.4
3427.14821	*Citrus sinensis* photosystem II reaction center W protein, chloroplastic (LOC102629478)	0	+ 2.1
3427.14577	*Citrus clementina* photosystem I reaction center subunit VI−2, chloroplastic (LOC18037749)	0	+ 2
3427.24274	*Citrus sinensis* ATP-dependent zinc metalloprotease FTSH 6, chloroplastic-like (LOC102613766)	0	−2
Carbon metabolism			
3427.5908	*Citrus clementina* ribose−5-phosphate isomerase 4 (LOC18051277)	0	+ 2.5
3427.22655	*Citrus clementina* ATP-dependent 6-phosphofructokinase 3 (LOC18056149)	0	−5.4
3427.1636	*Citrus clementina* transketolase, chloroplastic (LOC18043574)	0	−5.3
3427.26876	*Citrus clementina* pyruvate dehydrogenase E1 component subunit alpha, mitochondrial (LOC18045003)	0	−3.8
3427.19387	*Citrus clementina* 6-phosphogluconolactonase 1 (LOC18042243)	0	−2.9
Osmolyte			
3427.23455	*Citrus clementina* alpha-amylase (LOC18043125)	0	+ 4.9
3427.5062	*Citrus sinensis* proline dehydrogenase 2, mitochondrial (LOC102606965)	0	−5.8
3427.1673	*Citrus clementina* branched-chain-amino-acid aminotransferase 2, chloroplastic (LOC18040648)	0	−5.4
3427.20155	*Citrus clementina* trehalose-phosphate phosphatase F (LOC18049897)	0	−2.7
3427.7854	*Citrus clementina* alpha,alpha-trehalose-phosphate synthase [UDP-forming] 11 (LOC18054628)	0	−2.2
3427.24565	*Citrus clementina* galactinol–sucrose galactosyltransferase 2 (LOC18031328)	0	−2.9
3427.19532	*Citrus clementina* galactinol–sucrose galactosyltransferase 6 (LOC18055822)	0	−2.7

3.6.6. Osmolyte

Several genes involved in the metabolism of osmolytes such as proline, trehalose, BCAAs, and raffinose were found to be downregulated, whereas *C. clementina* alpha-amylase, which plays a critical role in the breakdown of starches into simpler sugars, was upregulated (Table 6).

3.6.7. Cell wall metabolism

Several genes involved in the synthesis of cellulose and hemicellulose were found to be upregulated. Similarly, multiple genes associated with cell wall biogenesis and modification were upregulated. Notably, two efflux-type boron transporters were found to be upregulated. *C. sinensis* boron transporter 1-like (BOR1) and *C. clementina* boron transporter 4 (BOR4) are required for efficient xylem loading of boron, which is essential for maintaining the integrity of plants' cell walls [99].

Additionally, genes related to wax biosynthesis were also upregulated. Notably, *C. sinensis* 3-ketoacyl-CoA synthase 10 (KCS10), a rate-limiting enzyme in the biosynthesis of very long-chain fatty acids (VLCFAs), which are crucial for wax production and drought tolerance [100], was upregulated.

Furthermore, genes involved in xylem formation and differentiation were found to be upregulated. Specifically, *C. sinensis* xylan O-acetyltransferase 1-like (ESK1), which is essential for the formation of functional xylem required for water transport to aerial tissues, was upregulated. This gene plays a key role in maintaining water economy, especially under drought conditions [101–103]. Additionally, *C. clementina* microtubule-associated protein 70–5 (MAP70.5), which is essential for the normal banding pattern of the secondary cell wall and for the proper development of xylem tracheary elements [104], was also found to be upregulated (Table 7).

3.6.8. ROS scavenging

As shown in Table 8, several genes involved in enzymatic ROS scavenging were identified. These include a *C. sinensis* superoxide dismutase (SOD) gene and two catalase (CAT) genes. SOD rapidly converts superoxide radicals ($\cdot O_2^-$) into H_2O_2, which is then broken down into water and oxygen by CAT and peroxidases [105,106]. In addition, multiple glutathione S-transferase (GST) genes were identified. GSTs are known to play key roles in plant adaptation to abiotic stress, pathogen defence, and the detoxification of harmful compounds [107–111]. Among these, dehydroascorbate reductase 2 (DHAR2), an enzyme involved in ascorbate recycling, has been shown to improve drought tolerance in *Arabidopsis* [112]. A 2-Cys peroxiredoxin (Prx), a thiol-based peroxidase that reduces H_2O_2 and organic hydroperoxides, was also identified. These enzymes contribute to drought tolerance by enhancing ROS scavenging activity, as demonstrated in tobacco [113] and rice [114]. Finally, two thioredoxins (Trxs) and one NADPH-dependent thioredoxin reductase (NTRC) were identified. Trxs are small oxidoreductases that serve as hydrogen donors to target proteins [115]. Overexpression of NTRA, another thioredoxin reductase, has been linked to improved oxidative and drought tolerance in *Arabidopsis* by regulating ROS levels [116]. Notably, all these genes were found to be upregulated in the present study. Specifically, transcript levels of the *SOD*, *CATs*, *GSTs* and *DHAR2* genes, as well as the *2-Cys Prx*, *Trxs* and *NTRC* loci, showed significant induction in primed plants under drought conditions.

3.7. WGCNA analysis

The application of WGCNA based on the expression data of 4369 unigenes belonging to the Priming Effect (PE) comparison, considering an FPKM > 1 threshold, aimed to establish correlations between MDA or H_2O_2 levels and gene expression patterns. Using the parameters and thresholds indicated in the Materials and Methods section, these genes were grouped into seven co-expressed modules, each represented by a

Table 7
List of DEGs related to cell wall metabolism during drought stress response identified in PE comparison.

Cluster ID	Database description	Evalue	log_2 fold change
Cell wall metabolism			
Cellulose biosynthesis			
3427.3035	*Citrus clementina* cellulose synthase A catalytic subunit 8 [UDP-forming] (LOC18053215)	0	+ 5.8
3427.15115	*Citrus clementina* protein IRX15-LIKE (LOC18035694)	0	+ 5
3427.4844	*Citrus sinensis* cellulose synthase A catalytic subunit 7 [UDP-forming] (LOC102616000)	0	+ 3.8
3427.23480	*Citrus clementina* beta−1,4-xylosyltransferase IRX9 (LOC18039260)	0	+ 3.8
3427.10311	*Citrus sinensis* cellulose synthase A catalytic subunit 4 [UDP-forming] (LOC102619893)	0	+ 3.5
3427.5582	*Citrus sinensis* cellulose synthase A catalytic subunit 3 [UDP-forming] (LOC102611367)	0	+ 2.4
Cell wall biogenesis and modification			
3427.8428	*Citrus sinensis* xyloglucan endotransglucosylase/hydrolase protein 31 (LOC102630992)	0	+ 4.9
3427.29684	*Citrus clementina* endoglucanase 24 (LOC18035044)	0	+ 4.9
3427.15489	*Arabidopsis thaliana* pectin methyltransferase QUA3 (Q93W95)	2.81E−08	+ 2.5
3427.14637	*Citrus sinensis* pectin acetylesterase 10-like (PAE10) (LOC102619995)	0	+ 2.5
3427.24555	*Citrus clementina* protein trichome birefringence-like 3 (LOC18039470)	0	+ 7.4
3427.3931	*Citrus sinensis* protein trichome birefringence-like 34 (LOC102627956)	0	+ 6.8
3427.16214	*Citrus sinensis* pectinesterase/ pectinesterase inhibitor 12 (LOC102609650)	0	+ 4.8
3427.8952	*Citrus clementina* chitinase-like protein 2 (LOC18031389)	0	+ 4.8
2910.0	*Citrus clementina* UDP-glucuronate:xylan alpha-glucuronosyltransferase 2 (LOC18040604)	0	+ 4.7
3427.1248	*Citrus sinensis* UDP-glucuronate:xylan alpha-glucuronosyltransferase 1 (LOC102610419)	0	+ 3.9
3427.11864	*Citrus sinensis* glucomannan 4-beta-mannosyltransferase 9 (LOC102616802)	0	+ 3.3
3427.20051	*Citrus sinensis* boron transporter 1-like (BOR1) (LOC102618488)	0	+ 3.3
3427.3303	*Citrus clementina* boron transporter 4 (BOR4) (LOC18036378)	0	+ 2.0
Wax biosynthesis			
3427.21272	*Citrus sinensis* fatty acyl-CoA reductase 2, chloroplastic-like (LOC102629259)	0	+ 7
3427.15660	*Citrus sinensis* 3-ketoacyl-CoA synthase 10 (KCS10) (LOC102627644)	0	+ 2.6
Xylem and phloem			
3427.9121	*Citrus sinensis* laccase−4-like (LOC102620940)	0	+ 5.3
3427.6991	*Citrus clementina* laccase−17 (LOC18034930)	0	+ 4.9
3427.4478	*Citrus sinensis* xylan O-acetyltransferase 1-like (ESK1) (LOC102626227)	0	+ 3.4
3427.17611	*Citrus sinensis* thermospermine synthase ACAULIS5-like (LOC102622802)	0	+ 3.3
3427.10901	*Citrus sinensis* polyamine oxidase 5 (LOC102609290)	0	+ 2.8
3427.13049	*Citrus sinensis* rho GTPase-activating protein 3 (ROPGAP3) (LOC102615569)	0	+ 2.7
3427.6163	*Citrus clementina* microtubule-associated protein 70–5 (MAP70.5) (LOC18050634)	0	+ 2.4

Table 8
List of DEGs related to ROS scavenging identified in the PE comparison.

Cluster ID	Database description	Evalue	log_2 fold change
3427.13306	*Citrus sinensis* superoxide dismutase [Cu-Zn], chloroplastic (SOD) (LOC102626642)	0	+ 1.9
3427.15091	*Citrus clementina* catalase (LOC18041273)	9.02E−81	+ 1.4
3427.13482	*Citrus sinensis* catalase-like (LOC102615999)	0	+ 1.4
3427.15858	*Citrus clementina* glutathione S-transferase DHAR2 (LOC18044375)	6.82E−170	+ 1.8
3427.19575	*Citrus clementina* glutathione S-transferase U7 (LOC18033889)	0	+ 1.7
3427.15830	*Citrus sinensis* glutathione S-transferase-like (LOC102624760)	0	+ 1.7
3427.3223	*Citrus sinensis* glutathione S-transferase U8-like (LOC102622765)	0	+ 1.6
3427.13555	*Citrus sinensis* peroxiredoxin−2E, chloroplastic (LOC102616506)	0	+ 1.7
3427.13445	*Citrus sinensis* 2-Cys peroxiredoxin BAS1, chloroplastic (LOC102619222)	0	+ 1.0
3427.15107	*Citrus clementina* thioredoxin-like protein CDSP32, chloroplastic (LOC18040800)	0	+ 1.4
3427.17821	*Citrus clementina* thioredoxin-like 4, chloroplastic (LOC18042042)	0	+ 1.4
3427.15922	*Citrus clementina* thioredoxin reductase NTRC (LOC18031501)	0	+ 1.3

branch of the tree (Figure S5). The number of eigengenes in different modules is reported in Figure S6. The black (3015) and tan (958) modules included the highest number of eigengenes, whereas the grey (31) and grey60 modules (41) gathered the lowest number of eigengenes (Figure S6). As shown in Fig. 8, illustrating the module–trait relationships, the black module exhibited significant negative correlations with MDA and H_2O_2 contents, showing −0.87 and −0.93 correlation coefficients, respectively. Similarly, the cyan module displayed a significant negative correlation solely with H_2O_2 (-0.71), whereas the tan module exhibited significant correlations with MDA and H_2O_2 contents, showing + 0.85 and + 0.92 correlation coefficients, respectively. On the contrary, the tan module showed significant positive correlations with MDA and H_2O_2 contents, showing + 0.85 and + 0.92 correlation coefficients, respectively. (Fig. 8). Since WGCNA correlates gene expression values with trait values, genes within modules that positively correlate with the traits are downregulated in the PE comparison, which exhibits low MDA and H_2O_2 levels. Conversely, genes in modules that negatively correlate with the traits are upregulated in the PE comparison.

In the WGCNA analysis, GS represents the correlation between a gene and a specific trait, whereas MM measures the correlation between an individual gene and the module eigengene. By applying a filtering threshold of MM and GS values ≥ 0.65, the black module contained 2140 eigengenes associated with H_2O_2 and 1907 eigengenes associated with MDA. Notably, within this module, only 12 eigengenes were uniquely correlated with MDA, while 245 were exclusively correlated with H_2O_2 (Fig. 9A). In the tan module, which positively correlates with both traits, 832 eigengenes were associated with H_2O_2 and 750 with MDA. Of these, 1 eigengene was uniquely correlated with MDA, while 83 were exclusively correlated with H_2O_2 (Fig. 9B).

3.7.1. GO enrichment of WGCNA modules

The GO enrichment analyses of the filtered eigengenes within each module (correlating with one or both traits) were performed in order to identify biological processes and pathways linked to drought stress tolerance in primed plants.

Fig. 10 shows the most significantly enriched GO terms for eigengenes in the black module associated with H_2O_2. The genes in this

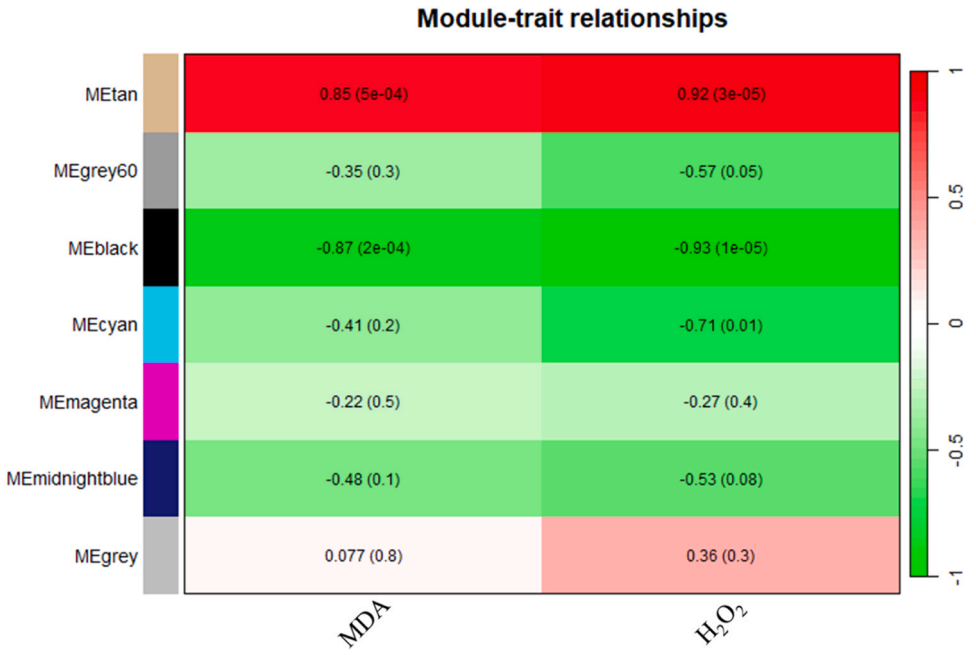

Fig. 8. Heatmap of the correlation between modules and malondialdehyde (MDA) and hydrogen peroxide (H_2O_2) levels.

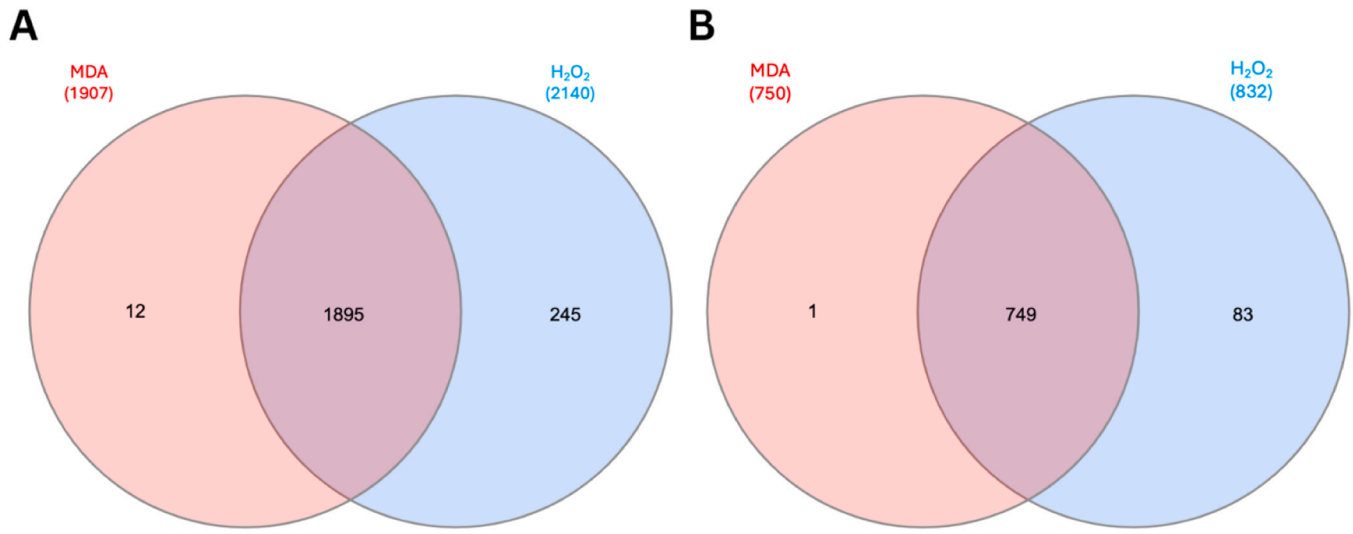

Fig. 9. Venn diagram showing the number of eigengenes correlated with either malondialdehyde (MDA) or hydrogen peroxide (H_2O_2) within the black (A) and tan (B) modules after applying a filtering threshold of MM and GS values ≥ 0.65.

module exhibit a negative correlation with the traits (Fig. 8), indicating their upregulation in the PE comparison. The Molecular Function category (Fig. 10A) is enriched with terms related to cell signalling, stress responses, growth regulation, and metabolic pathways. The Biological Processes category (Fig. 10B) is mostly enriched in terms related to plant growth, development, morphogenesis, and photosynthesis. The enrichment analysis revealed minimal differences between the eigengene lists of the black module correlating with MDA and H_2O_2.

Fig. 11 shows the most significantly enriched GO terms for eigengenes in the cyan module associated with H_2O_2. The Molecular Function category (Fig. 11A) is enriched with terms associated with signalling, ATP-dependent phosphorylation, and nucleotide metabolism. The Biological Processes category (Fig. 11B) is enriched in terms related to post-translational modifications, which is a crucial regulatory mechanism in signal transduction. The only two terms found in the Cellular Component category (Fig. 11C) related to membrane-associated processes are also present in Fig. 5C.

Fig. 12 shows the most significantly enriched GO terms for eigengenes in the tan module associated with MDA. Notably, all enriched terms in the Biological Processes category (Fig. 12B) are associated with hypoxia-related responses, which play a crucial role in plant adaptation to low oxygen conditions, such as those found in compacted or waterlogged soil. For this module, the enrichment analysis of the eigengenes correlated with H_2O_2 yielded no significant results.

4. Discussion

Abiotic and biotic stresses significantly influence plant and crop growth, as well as their reproductive processes. Understanding the complex molecular mechanisms underlying cellular responses to these stresses is essential for addressing the challenges posed by climate change and ensuring food security. Recent studies focused on examining

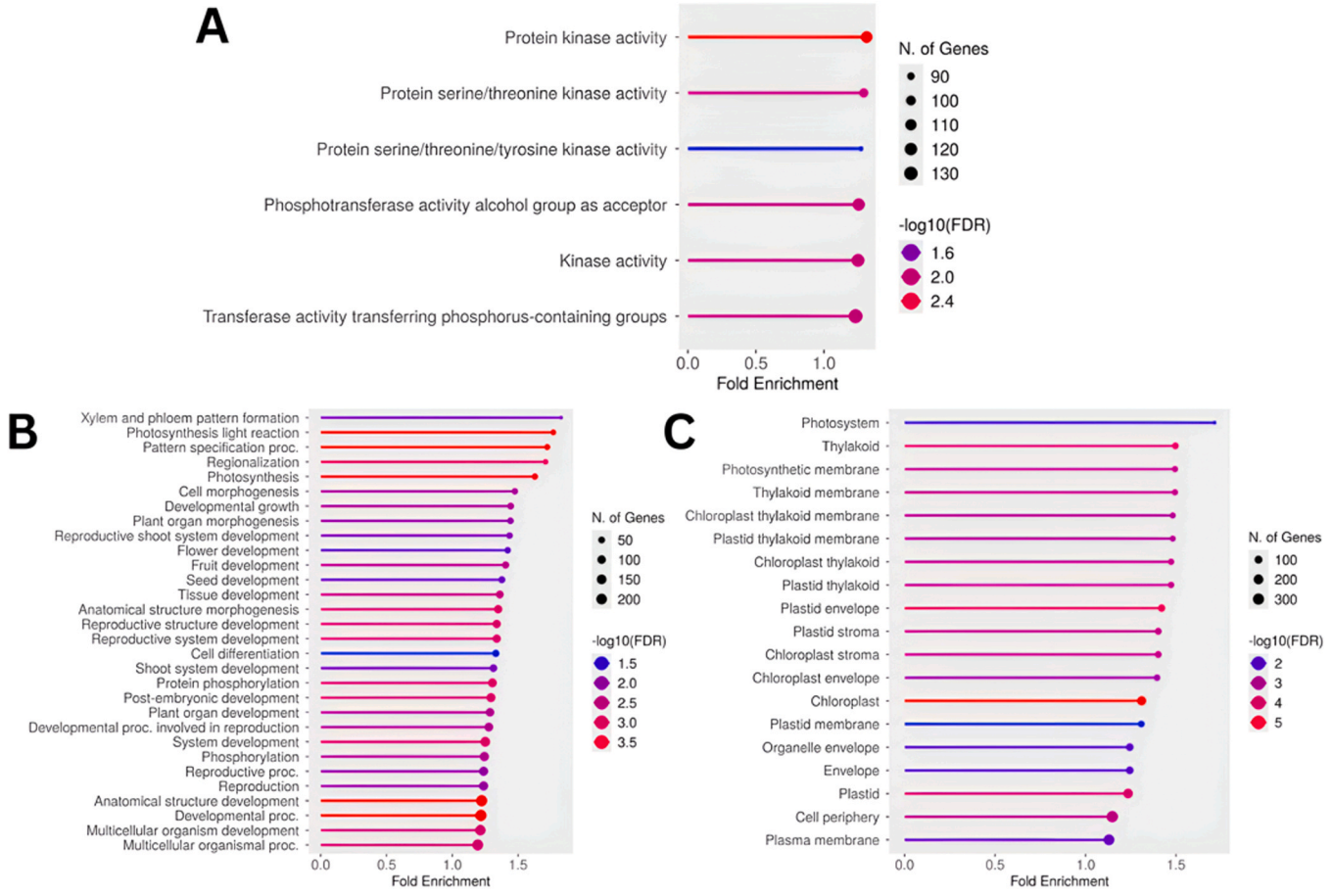

Fig. 10. Lollipop plot showing the Gene Ontology (GO) enrichment analysis for the eigengenes in the black module correlating with H_2O_2. (A) Molecular Function, (B) Biological Process, and (C) Cellular Component categories. The X-axis represents the Fold Enrichment, while the Y-axis lists the enriched GO terms. The colour gradient of the dots represents the -log10(FDR), with darker colours indicating higher statistical significance (lower FDR values). The size of the dots corresponds to the number of genes associated with each GO term.

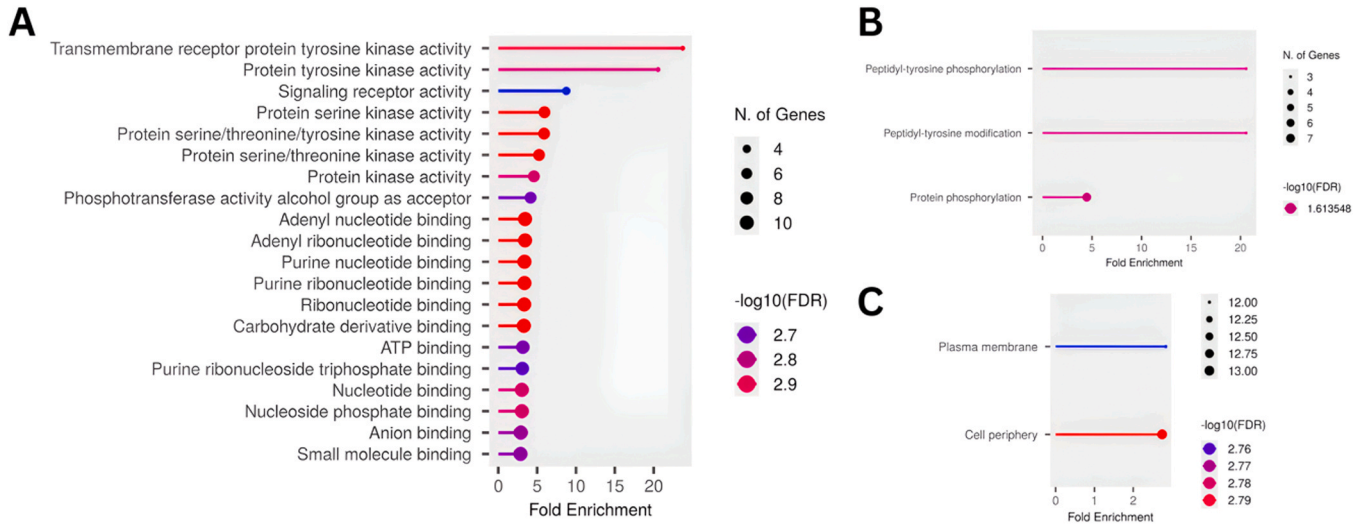

Fig. 11. Lollipop plot showing the Gene Ontology (GO) enrichment analysis for the eigengenes in the cyan module correlating with hydrogen peroxide (H_2O_2). (A) Molecular Function, (B) Biological Process, and (C) Cellular Component categories. The X-axis represents the Fold Enrichment, while the Y-axis lists the enriched GO terms. The colour gradient of the dots represents the -log10(FDR), with darker colours indicating higher statistical significance (lower FDR values). The size of the dots corresponds to the number of genes associated with each GO term.

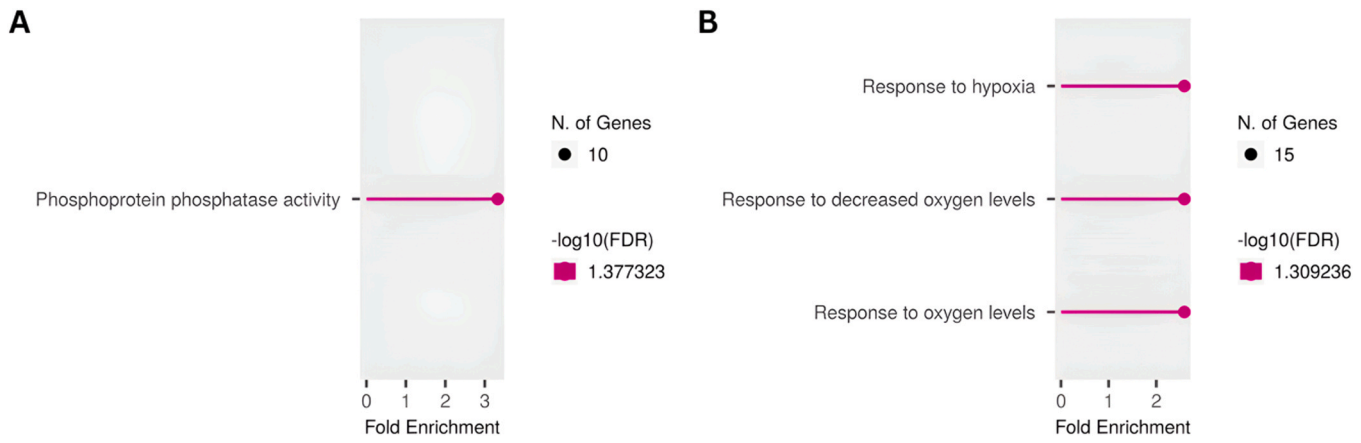

Fig. 12. Lollipop plot showing the Gene Ontology (GO) enrichment analysis for the eigengenes in the tan module correlating with malondialdehyde (MDA). (A) Molecular Function and (B) Biological Process categories. The X-axis represents the Fold Enrichment, while the Y-axis lists the enriched GO terms. The colour gradient of the dots represents the -log10(FDR), with darker colours indicating higher statistical significance (lower FDR values). The size of the dots corresponds to the number of genes associated with each GO term.

the transcriptome changes in various *Citrus* rootstock genotypes under drought conditions using RNA-seq analysis [117,118]. For instance, Gonçalves et al. [117] reported activation of genes related to the cell wall, sugar and antioxidant metabolism, stress responses, transcriptional regulation, and ABA signalling, along with repression of genes involved in starch metabolism, light reactions, and ethylene signalling in drought-tolerant 'Rangpur' lime. These results align with those found in this work except for starch metabolism and light reactions, which showed opposite trends. More recently, transcriptomic analysis on two *Citrus* rootstock genotypes, Carrizo citrange and Bitters (C22), subjected to PEG-induced drought stress in hydroponic conditions was performed [37]. The study revealed that Carrizo citrange exhibited higher sensitivity to drought, as corroborated by the observed significant transcriptomic alterations, whereas Bitters (C22) showed only minimal transcriptomic changes, indicating a more resilient response. Carrizo's response to drought stress involved both the activation of ABA-mediated pathways and an upregulation of genes related to proline, glycine betaine, and raffinose family oligosaccharides (RFO) biosynthesis, as well as the downregulation of polyamine catabolic genes. Notably, the modulation of genes associated with cell wall metabolism played a crucial role in Carrizo's drought response [37]. Taken as a whole, this response typology could be hinged as drought-sensitive behaviour. Additionally, a proteomic study on the effect of SNP priming in sour orange (*Citrus aurantium* L.) under PEG-induced drought stress reported enhanced tolerance one month after treatment, in agreement with our findings [42]. This study also observed the upregulation of proteins involved in photosystem II repair, consistent with our results. Moreover, the downregulation of ROS-detoxifying enzymes in non-primed plants was linked to increased drought sensitivity, which aligns with the upregulation of ROS-scavenging genes observed in SNP-treated plants in our study. To date, this is the only study specifically addressing the role of SNP in drought tolerance in citrus. However, its effects have been explored in other species. For example, SNP application has been shown to enhance drought tolerance in *Silybum marianum* L. (*S. marianum*) [41], lettuce (*Lactuca sativa*) [40], tomato (*Solanum lycopersicum*) [119], and strawberry (*Fragaria* × *ananassa*) [120].

Considering its highest potential to cope with drought [37], this work presents the results of RNA sequencing and the *de novo* assembly of Bitters (C22) plants treated with SNP, a NO-donor, followed by drought stress exposure induced by withholding water. The aim is to deepen our understanding of the molecular mechanisms underlying priming effects in citrus plants in response to drought stress conditions.

The non-primed stressed plants (ST) were severely affected by the drought, as evidenced by both their phenotype and significantly elevated MDA and H_2O_2 levels. In comparison, the control plants (CK and SNP-CK) exhibited no stress symptoms and maintained very low MDA and H_2O_2 levels, indicating that the priming treatment had no collateral effects under normal watering conditions. Notably, the primed stressed plants (SNP-ST) displayed a healthy phenotype, similar to the control samples, suggesting that the priming pretreatment enhanced tolerance to the successively imposed drought stress. Furthermore, the PCA analysis revealed a very tight clustering of samples within their respective treatments, indicating minimal variation among replicates. Interestingly, both control treatments clustered closely together, suggesting no significant differences in transcriptomic rearrangements under non-stress conditions. These results indicate that the priming treatment was effective in enhancing tolerance to drought stress, also having minimal impact under normal watering conditions.

Differential gene expression analysis revealed an extremely low number of DEGs between the two control treatments (CK and SNP-CK), which aligns with the minimal differences observed in earlier analyses and confirms that the priming treatment had no significant effect under normal watering conditions also at the transcriptomic level. Despite the extremely low number of DEGs, within the SNP-CK vs. CK comparison, the GO enrichment analysis yielded noteworthy results as all the enriched terms were associated with cell wall biogenesis, modification, and polysaccharide metabolism, suggesting that the priming treatment specifically influenced cell wall regulation under normal watering conditions. This indicates a targeted transcriptional response, potentially preparing the plant for structural reinforcement or stress adaptation.

The substantial difference in the number of DEGs between the ST vs CK (9393) and SNP-ST vs SNP-CK (3556) comparisons indicates that primed plants experienced fewer transcriptomic changes than non-primed plants after 34 days of drought stress. This suggests that a smaller number of DEGs was sufficient for primed plants to achieve drought tolerance. The "comparison of comparisons" (PE), which examined the differences in DEG profiles between the two comparisons [(SNP-ST vs SNP-CK) vs (ST vs CK)], helped to identify the set of DEGs specifically induced by priming under drought stress (the Priming Effect). Therefore, the PE comparison was selected for further analysis. The GO enrichment analysis of the DEGs from the PE comparison revealed the enrichment of terms associated with diverse biological pathways, including photosynthesis, hormone regulation, cell wall regulation, xylem development, and responses to external, biotic, and chemical stimuli. This suggests a broader transcriptional reprogramming in response to the priming treatment under drought stress conditions. Interestingly, unlike the PE comparison, no GO terms related to xylem formation and differentiation were observed in the SNP-CK vs CK

comparison, despite the fact that xylem development requires extensive cell wall modification, biosynthesis, and remodelling, which were well represented in this comparison. This suggests that the priming treatment influenced cell wall metabolism, but it did not induce xylem differentiation under normal watering conditions. However, the enrichment of these terms in the PE comparison indicates that SNP priming regulates xylem formation and differentiation specifically in response to water deficit, potentially as an adaptive mechanism to enhance drought tolerance by optimizing water transport and structural reinforcement under stress conditions.

While THESEUS1, FERONIA, and WAK2-like are traditionally linked to general cell elongation and expansion, the cellular processes they regulate, such as cell wall remodelling and integrity sensing, are also essential for xylem differentiation. This aligns with the upregulation of genes specifically involved in xylem formation. Consequently, the increased expression of these genes in primed plants under stress conditions may indicate adaptive modifications in xylem development. Additionally, the deregulation of genes related to various stress responses, such as the upregulation of CRPK1, a negative regulator of freezing tolerance [56], MSL10, a mechanosensitive channel that converts mechanical force into ion flux [57], and HPCA1, a receptor protein kinase crucial for stomatal closure [60], highlights a complex activation of stress response pathways. Among the genes involved in calcium signalling [121], MCA1, a major plant mechanosensitive Ca^{2+} influx channel, was found to be upregulated. Its known role in cold tolerance in *Arabidopsis* [59] and its proposed function in sensing hydraulic pressure changes under dehydration stress [58] suggest that it may contribute to the enhanced drought tolerance observed in SNP-primed plants. In this respect, the Ca^{2+} transporter *TaNCL2-A*, well known for its involvement in various abiotic stresses, including drought, and for its interaction with ABA [122] was not identified in our comparisons. The down-regulation of negative regulators of PTI in response to multiple PAMPs, such as PUB24-like and PUB23-like [61], alongside a receptor kinase associated with *Phytophthora* resistance, H_2O_2 production, and cell death (IX.1-like) [63], further indicates that priming triggered signalling pathways linked to the plant's responses to various stresses, including biotic stress. Furthermore, the downregulation of the bidirectional sugar transporter SWEET15, which has been proposed as a molecular link integrating environmental stress responses with the senescence process, may contribute to the tolerant phenotype of primed plants. Notably, SWEET15-overexpressing transgenic plants (35S:SWEET15) exhibit accelerated senescence and increased sensitivity to salt stress, whereas SWEET15-deficient mutants display enhanced tolerance to high salinity [123].

Regarding hormone regulation, the repression of key ethylene biosynthesis and signalling genes, such as ACS1, ACO, and the receptor ETR2, suggests that ethylene production could be reduced. Although ethylene is a key signalling molecule in abiotic stress tolerance, its role remains unclear. Hence, some studies report a positive impact of ethylene or its precursor, 1-aminocyclopropane-1-carboxylate (ACC), on stress tolerance [124–126], whereas other researches highlight the negative role of ethylene in coping with stressful conditions [127–129]. Therefore, the observed down-regulation of ethylene in the tolerant, primed plants suggests that ethylene might not be a significant factor in the observed drought tolerance. In contrast, the expression of genes involved in auxin biosynthesis and signalling activity was clearly enhanced. Notably, the upregulation of MES17, which hydrolyses MeIAA into the active form of auxin (IAA) [71], and HLS1, which contributes to elevate free IAA levels [65], along with the induction of genes involved in auxin signalling and transport, suggest a key role for auxin in promoting SNP-induced tolerance to the stress conditions. Although the role of ABA in abiotic stress responses, particularly drought, is well established [130], no genes directly involved in its biosynthesis were identified, suggesting that both primed and non-primed plants regulated ABA levels similarly. However, we observed the upregulation of RHA2A, a positive regulator of ABA signalling and responses to salt, osmotic stress [76], and drought [77]. Additionally, ARIA, whose overexpression enhances high-salinity tolerance in *Arabidopsis* [75], was also upregulated. Furthermore, the downregulation of KEG, a negative regulator of ABA signalling [78], highlights these genes as potential contributors to enhanced drought tolerance. Regarding GA, the upregulation of GAMT2 suggests the active degradation of gibberellins through their methylation [79] under stress conditions. Additionally, the upregulation of RGL1-like, a repressor of GA signalling, further supports the negative regulation of GA in the tolerant phenotype. DELLAs, including RGL1, have been shown to repress ROS levels by regulating the transcription of genes encoding ROS detoxification enzymes, thereby enhancing tolerance to both biotic and abiotic stresses [131].

Transcription factors are pivotal regulators that govern the expression of numerous target genes, profoundly influencing drought tolerance in plants by translating stress signals into appropriate cellular responses. In line with the aforementioned deregulation of hormone signalling pathways, TFs associated with different stress responses were concordantly deregulated. Hence, ERF1B, which integrates ethylene and jasmonate signals to modulate defence response genes [81,82], was downregulated. Additionally, GATA4, involved in regulating light-responsive genes [85], and CAMTA4, which plays a role in positively regulating the general stress response via Ca^{2+} signalling [86], were upregulated. Furthermore, HDG11 was first isolated from *Arabidopsis* mutant with improved drought tolerance, and its overexpression in tobacco plants also conferred drought tolerance, which was associated with improved root architecture and reduced leaf stomatal density [87]. This suggests that HDG11 may play a critical role in the tolerant phenotype of primed plants. Double mutants of *FOUR LIPS* (FLP) and its paralog *MYB88* in *Arabidopsis* exhibited increased susceptibility to drought and high salinity, along with higher rates of water loss [92]. Therefore, the upregulation of *CsMYB124*, a homolog of *AtMYB88*, in primed plants may have contributed to enhanced tolerance to water scarcity. Meanwhile, several WRKY transcription factors, including WRKY 72A-like, which contributes to basal defence against root-knot nematodes and potato aphids [88], were notably downregulated, suggesting a shift in the plant's basal defence mechanisms under stress conditions.

Interestingly, both DREB2A and DREB3 were previously reported to be induced under PEG-induced drought stress in citrus [37]. In this study, however, only DREB3 was upregulated, whereas DREB2A was downregulated, suggesting that DREB3 may play a crucial role in contributing to drought tolerance under these specific conditions. Notably, several transcription factors involved in xylem formation and differentiation were identified. NAC76-like, which promotes xylem formation by enhancing the expression of secondary wall-associated genes [90], and NAC012 were upregulated. *Arabidopsis* plants overexpressing NAC012 exhibited increased cell-wall thickness in the xylem vessels [132]. Furthermore, MYB61, known to regulate xylem formation, xylem cell differentiation [91], and stomatal pore size independently of ABA [133], was also upregulated. The upregulation of SHORT-ROOT-like, essential for bundle sheath cell fate specification in leaves [96], reinforces the indication of global strong activation of genes promoting xylem development. Additionally, SCL7, which enhances the expression of stress-responsive genes, particularly under salt and drought stress [94], was upregulated. Given that the Scarecrow gene family collaborates with SHORT-ROOT in regulating cell proliferation and bundle sheath cell fate specification [96], p. 23; [95], these findings highlight it as a promising candidate for drought tolerance.

The upregulation of genes associated with photosystems I and II indicates that the plants are likely trying to preserve or even boost light harvesting efficiency under stress conditions. In contrast, the downregulation of genes involved in the PPP and the Calvin cycle suggests that the plant is limiting growth and biomass accumulation. This could reflect a strategic reallocation of energy and resources, allowing the plant to cope with drought conditions more effectively. Furthermore, it has been shown that BCA-overexpressing plants (beta carbonic

anhydrase 1) exhibit an immediate increase in water use efficiency [98]. BCA1 functions early in the CO_2 signalling pathway, which regulates gas exchange between plants and the atmosphere. Therefore, its overexpression may contribute to the tolerant phenotype of primed plants.

Given these findings, we propose a model according to primed plants maintained an elevated light-harvesting activity, despite limiting growth and biomass accumulation in terms of carbon fixation. The energy produced as ATP molecules in the light could be likely reallocated to support metabolic pathways essential for drought response. The enrichment of the "ATP-dependent ABC transporters" among the KEGG categories aligns with the supposed increase in ATP production.

The upregulation of several genes involved in cellulose biosynthesis, cell wall biogenesis and modification, and wax biosynthesis suggests that the plants were actively reinforcing and remodelling their external barriers and structural integrity to withstand drought stress. Moreover, the upregulation of genes involved in xylem formation and differentiation highlights the vital role of xylem remodelling in conferring drought tolerance to primed plants. Therefore, genes like KCS10, a rate-limiting enzyme in the biosynthesis of very long-chain fatty acids (VLCFAs), essential for wax production and drought tolerance [100], ESK1, crucial for the formation of functional xylem and maintaining water economy under drought [101–103], and MAP70.5, which is essential for the proper development of xylem [104], emerge as key candidate genes contributing to the drought tolerance observed in primed plants.

Since the well-established role of osmoprotectants in maintaining cellular homeostasis and stabilising proteins and membranes during drought stress, the down-regulation of genes involved in the synthesis of osmolytes such as proline, trehalose, BCAAs, and raffinose suggests that the plants may have adopted an alternative response strategy. This indicates that osmolyte accumulation probably did not play a critical role in the drought tolerance observed in primed plants, and it might represent a signature of stress sensitivity, as observed in Carrizo [37].

Enzymatic antioxidants such as SOD, CAT, ascorbate peroxidase (APX), glutathione peroxidase (GPX), glutathione reductase (GR), monodehydroascorbate reductase (MDHAR), and DHAR have been shown to increase under drought stress in various plant species, as thoroughly reviewed by Das and [134]. This upregulation is often associated with significant reductions in H_2O_2 and MDA levels, indicating enhanced ROS detoxification. In addition, several studies have demonstrated that respiratory burst oxidase homolog (RBOH) genes exhibit differential expression and play a role in drought stress tolerance [135–137]. Although not all of these genes were detected in the present study as DEGs, the upregulation of several ROS-scavenging genes (Table 8) aligns well with the significant reductions in MDA and H_2O_2 observed in SNP-treated plants. These findings suggest that SNP priming enhances the antioxidant defence system, likely contributing to reduced oxidative damage. Additionally, Trx itself supports the reduced state of Prx, and Trx is maintained in its reduced form by thioredoxin reductase (TrxR) [138,139]. The NTRC/2-Cys Prx system, a chloroplast-localised H_2O_2-scavenging mechanism has been linked to improved oxidative and drought tolerance in *Arabidopsis* [116]. This interaction highlights the coordinated activity of thiol-based redox systems in maintaining ROS homeostasis, further supporting the role of these genes in the improved stress tolerance observed in primed plants.

The application of WGCNA enabled the identification of genes whose expression showed positive or negative correlations with the levels of MDA and/or H_2O_2. Accordingly, GO enrichment analysis performed on the list of eigengenes, derived from WGCNA and grouped within modules significantly correlating with MDA and/or H_2O_2 traits, identified specific terms not observed in the general GO enrichment analysis performed on the list of DEGs belonging to the PE comparison, including priming-induced DEGs under drought stress condition (Fig. 5). Furthermore, the analysis discovered pathways in which the genes belonging to the most significantly associated modules are involved. The black module, which contains genes upregulated in the PE comparison and inversely correlated with both MDA and H_2O_2, showed enrichment for several terms also observed in the PE comparison. Specifically, a strong representation of development-related terms and terms associated with photosynthetic compartments was observed, strengthening the results of the general PE comparison enrichment. The strong enrichment of these terms, along with the observed downregulation of genes involved in energy production, reinforces the suggestion that primed plants may be channelling resources toward protective and repair mechanisms rather than rapid growth. This finding aligns with their increased drought tolerance, as evidenced by their healthier phenotype. The cyan module, inversely correlated with H_2O_2 levels, revealed strong enrichment in ATP-dependent phosphorylation and nucleotide metabolism-related terms, which were not observed in the PE comparison enrichment. These terms are generally associated with fundamental cellular processes, including energy transfer, signal transduction, and nucleic acid metabolism. This result suggests that primed plants exhibited enhanced metabolic activity compared to non-primed plants during drought. The tan module, positively correlated with H_2O_2, contains genes downregulated in the PE comparison and was enriched exclusively in terms associated with hypoxia-related responses. Since these genes were highly expressed in non-primed stressed plants (ST), this finding suggests that prolonged water deprivation led to low oxygen availability in the soil, activating hypoxia-responsive pathways in the affected plants. Moreover, their downregulation in the PE comparison indicates that these pathways are not involved in the tolerance observed in primed plants.

The results offer valuable insights into the molecular responses of SNP-induced drought stress tolerance in *Citrus*. However, future studies including physiological validation would help to further support these findings.

5. Conclusion

In this study, Bitters (C22) citrus rootstock plants were subjected to SNP-induced priming followed by drought stress to investigate the molecular mechanisms underlying priming effects during water scarcity. Visual inspection of the phenotype, along with MDA and H_2O_2 measurements, clearly demonstrated that SNP-induced priming enhanced the plants' resilience. Under control conditions, priming treatment alone elicited minimal changes in both plant phenotype and transcriptomic profile, with alterations limited exclusively to cell wall metabolism. The regulation of responses to various biotic and abiotic stresses was observed in primed plants, as suggested by the deregulation of genes associated with signalling pathways and TFs involved in diverse stress responses. In particular, genes involved in ethylene biosynthesis and signalling were repressed, whereas those implicated in auxin biosynthesis and signalling were induced due to the priming effect. It appears that primed plants aimed to maintain their photosynthetic efficiency under stress conditions while limiting growth and biomass accumulation, likely reallocating energy and resources toward defensive pathways. The downregulation of genes involved in osmoprotectant biosynthesis suggests that these compounds may not play a central role in SNP-induced drought tolerance. Likewise, the induction of hypoxia-related responses likely did not contribute to SNP-induced drought tolerance, as evidenced by the WGCNA results. In contrast, the reinforcement and remodelling of external barriers, along with xylem modification and ROS-scavenging, may have been critical in enhancing or conferring drought tolerance, as indicated by the upregulation of numerous genes triggered in primed plants by the stress conditions. Therefore, the priming treatment followed by drought stress appeared to regulate responses to a broad spectrum of stresses. Based on global transcriptomic analysis, the most significant outcomes of this regulation were high photosynthetic efficiency, a strategic reallocation of energy and resources, increased antioxidant power, and the reinforcement and remodelling of external barriers and xylem vessels. These findings offer valuable insights into the effectiveness of SNP-priming in enhancing drought tolerance and the molecular mechanisms triggered by this

treatment, highlighting potential candidate genes for improving drought resilience in *Citrus*.

Funding sources

This research was funded by "Miglioramento delle produzioni agroalimentari mediterranee in condizioni di carenza di risorse idriche—WATER4AGRIFOOD"—Code: ARS01_00825, PON "RICERCA E INNOVAZIONE" 2014–2020, Azione II—Obiettivo Specifico 1b, CUP: B64I20000160005, which did not cover the open access fee.

CRediT authorship contribution statement

Emanuele Scialò: Data curation, Formal analysis, Investigation, Methodology, Resources, Software, Validation, Writing – original draft, Writing – review & editing. **Angelo Sicilia:** Formal analysis, Methodology, Resources, Software, Visualisation, Writing – review & editing. **Angela Roberta Lo Piero:** Conceptualization, Data curation, Funding acquisition, Methodology, Supervision, Writing – review & editing.

Declaration of Competing Interest

The authors declare that they have no known competing financial interests or personal relationships that could have appeared to influence the work reported in this paper.

Acknowledgements

We gratefully acknowledge "Vivai Messina Filippo, Piante Agrumi ed Olivi" for providing high-quality plant materials.

Appendix A. Supporting information

Supplementary data associated with this article can be found in the online version at doi:10.1016/j.cpb.2025.100508.

Data availability

Raw sequencing data has been deposited in the NCBI SRA (https://www.ncbi.nlm.nih.gov/sra) and it will be publicly available upon completion of submission, reference number PRJNA1231020.

References

[1] C. Rosenzweig, J.W. Jones, J.L. Hatfield, A.C. Ruane, K.J. Boote, P. Thorburn, J. M. Antle, G.C. Nelson, C. Porter, S. Janssen, S. Asseng, B. Basso, F. Ewert, D. Wallach, G. Baigorria, J.M. Winter, The Agricultural Model Intercomparison and Improvement Project (AgMIP): protocols and pilot studies, Agricult. For. Meteorol. Agric. Predict. Using Clim. Model Ensembles 170 (2013) 166–182, https://doi.org/10.1016/j.agrformet.2012.09.011.

[2] A. Gupta, A. Rico-Medina, A.I. Caño-Delgado, The physiology of plant responses to drought, Science 368 (2020) 266–269, https://doi.org/10.1126/science.aaz7614.

[3] Y. Osakabe, K. Osakabe, K. Shinozaki, L.-S.P. Tran, Response of plants to water stress, Front. Plant Sci. 5 (2014), https://doi.org/10.3389/fpls.2014.00086.

[4] I. Puglisi, E. Nicolosi, D. Vanella, A.R. Lo Piero, F. Stagno, D. Saitta, G. Roccuzzo, S. Consoli, A. Baglieri, Physiological and biochemical responses of orange trees to different deficit irrigation regimes, Plants 8 (2019) 423, https://doi.org/10.3390/plants8100423.

[5] P. Romero, J.M. Navarro, J. Pérez-Pérez, F. García-Sánchez, A. Gómez-Gómez, I. Porras, V. Martinez, P. Botía, Deficit irrigation and rootstock: their effects on water relations, vegetative development, yield, fruit quality and mineral nutrition of Clemenules mandarin, Tree Physiol. 26 (2006) 1537–1548, https://doi.org/10.1093/treephys/26.12.1537.

[6] H. Abu Glion, S. Alkalai-Tuvia, M. Zaaroor-Presman, D. Chalupowicz, M. Zanbar, M. Amichai, S. Cohen, T. Shemer, S. Sarig, E. Fallik, Effects of rootstock/scion combination and two irrigation water qualities on cherry tomato yield and postharvest fruit quality, Horticulturae 5 (2019) 35, https://doi.org/10.3390/horticulturae5020035.

[7] L. Zhang, E. Marguerit, L. Rossdeutsch, N. Ollat, G.A. Gambetta, The influence of grapevine rootstocks on scion growth and drought resistance, Theor. Exp. Plant Physiol. 28 (2016) 143–157, https://doi.org/10.1007/s40626-016-0070-x.

[8] L. Aparicio-Durán, F.G. Gmitter Jr., J.M. Arjona-López, R. Calero-Velázquez, Á. Hervalejo, F.J. Arenas-Arenas, Water-Stress Influences on Three New Promising HLB-Tolerant Citrus Rootstocks, Horticulturae 7 (2021) 336, https://doi.org/10.3390/horticulturae7100336.

[9] L. López-Serrano, G. Canet-Sanchis, G. Vuletin Selak, C. Penella, A. San Bautista, S. López-Galarza, Á. Calatayud, Pepper Rootstock and Scion Physiological Responses Under Drought Stress, Front. Plant Sci. 10 (2019), https://doi.org/10.3389/fpls.2019.00038.

[10] Castle, W.S., Baldwin, J.C., Muraro, R.P., Littell, R., 2010. Performance of 'Valencia' Sweet Orange Trees on 12 Rootstocks at Two Locations and an Economic Interpretation as a Basis for Rootstock Selection. https://doi.org/10.21273/HORTSCI.45.4.523.

[11] D.D.S. Santana-Vieira, L. Freschi, L.A. Almeida, H. da, D.H.S. Moraes, D.M. de, Neves, L.M. Santos, F.Z. dos, Bertolde, W. Soares Filho, S. dos, M.A. Coelho Filho, A. Gesteira, S. da, Survival strategies of citrus rootstocks subjected to drought, Sci. Rep. 6 (2016) 38775, https://doi.org/10.1038/srep38775.

[12] M. Zhao, Q. Zhang, H. Liu, S. Tang, C. Shang, W. Zhang, Y. Sui, Y. Zhang, C. Zheng, H. Zhang, C. Liu, J. Chu, G. Jia, H. Wang, X. Liu, D. An, F. Zhu, H. Zhi, C. Wu, X. Diao, The osmotic stress–activated receptor-like kinase DPY1 mediates SnRK2 kinase activation and drought tolerance in Setaria, Plant Cell 35 (2023) 3782–3808, https://doi.org/10.1093/plcell/koad200.

[13] J. Shekhawat, S.K. Upadhyay, DPY1 as an osmosensor for drought signaling, Trends Plant Sci. 29 (2024) 616–619, https://doi.org/10.1016/j.tplants.2023.12.011.

[14] S. Tyagi, Shumayla, Y. Sharma, Madhu, A. Sharma, A. Pandey, K. Singh, S. K. Upadhyay, TaGPX1-D overexpression provides salinity and osmotic stress tolerance in Arabidopsis, Plant Sci. 337 (2023) 111881, https://doi.org/10.1016/j.plantsci.2023.111881.

[15] S. Tyagi, Shumayla, K. Singh, A. Pandey, S.K. Upadhyay, TaCCS1-B expression modulates copper, enzymatic antioxidants and polyphenols contents and provides abiotic stress tolerance in transgenic Arabidopsis, Physiol. Plant 176 (2024) e14645, https://doi.org/10.1111/ppl.14645.

[16] U. Conrath, Chapter 9 priming of induced plant defense responses. Advances in Botanical Research, Advances in Botanical Research. Academic Press, 2009, pp. 361–395, https://doi.org/10.1016/S0065-2296(09)51009-9.

[17] H. Ellouzi, K. Ben Hamed, M.A. Asensi-Fabado, M. Müller, C. Abdelly, S. Munné-Bosch, Drought and cadmium may be as effective as salinity in conferring subsequent salt stress tolerance in Cakile maritima, Planta 237 (2013) 1311–1323, https://doi.org/10.1007/s00425-013-1847-7.

[18] E. Sani, P. Herzyk, G. Perrella, V. Colot, A. Amtmann, Hyperosmotic priming of Arabidopsis seedlings establishes a long-term somatic memory accompanied by specific changes of the epigenome, Genome Biol. 14 (2013) R59, https://doi.org/10.1186/gb-2013-14-6-r59.

[19] Y. Zhao, X. Wei, Y. Long, X. Ji, Transcriptional analysis reveals sodium nitroprusside affects alfalfa in response to PEG-induced osmotic stress at germination stage, Protoplasma 257 (2020) 1345–1358, https://doi.org/10.1007/s00709-020-01508-x.

[20] V. Ziogas, G. Tanou, M. Belghazi, P. Filippou, V. Fotopoulos, D. Grigorios, A. Molassiotis, Roles of sodium hydrosulfide and sodium nitroprusside as priming molecules during drought acclimation in citrus plants, Plant Mol. Biol. 89 (2015) 433–450, https://doi.org/10.1007/s11103-015-0379-x.

[21] A. Savvides, S. Ali, M. Tester, V. Fotopoulos, Chemical Priming of Plants Against Multiple Abiotic Stresses: Mission Possible? Trends Plant Sci. 21 (2016) 329–340, https://doi.org/10.1016/j.tplants.2015.11.003.

[22] M. Khan, S. Ali, T.N.I. Al Azzawi, S. Saqib, F. Ullah, A. Ayaz, W. Zaman, The Key Roles of ROS and RNS as a Signaling Molecule in Plant–Microbe Interactions, Antioxidants 12 (2023) 268, https://doi.org/10.3390/antiox12020268.

[23] M. Simontacchi, A. Galatro, F. Ramos-Artuso, G.E. Santa-María, Plant survival in a changing environment: the role of nitric oxide in plant responses to abiotic stress, Front. Plant Sci. 6 (2015), https://doi.org/10.3389/fpls.2015.00977.

[24] M. Khan, T.N.I. Al Azawi, A. Pande, B.-G. Mun, D.-S. Lee, A. Hussain, B.-H. Lee, B.-W. Yun, The Role of Nitric Oxide-Induced ATILL6 in Growth and Disease Resistance in Arabidopsis thaliana, Front. Plant Sci. 12 (2021), https://doi.org/10.3389/fpls.2021.685156.

[25] W. Rahim, M. Khan, T.N.I. Al Azzawi, A. Pande, N.J. Methela, S. Ali, M. Imran, D.-S. Lee, G.-M. Lee, B.-G. Mun, Y.-S. Moon, I.-J. Lee, B.-W. Yun, Exogenously Applied Sodium Nitroprusside Mitigates Lead Toxicity in Rice by Regulating Antioxidants and Metal Stress-Related Transcripts, Int. J. Mol. Sci. 23 (2022) 9729, https://doi.org/10.3390/ijms23179729.

[26] N.K. Rolly, Q.M. Imran, M. Shahid, M. Imran, M. Khan, S.-U. Lee, A. Hussain, I.-J. Lee, B.-W. Yun, Drought-induced *AtbZIP62* transcription factor regulates drought stress response in Arabidopsis, Plant Physiol. Biochem. 156 (2020) 384–395, https://doi.org/10.1016/j.plaphy.2020.09.013.

[27] N. Correa-Aragunde, N. Foresi, L. Lamattina, Nitric oxide is a ubiquitous signal for maintaining redox balance in plant cells: regulation of ascorbate peroxidase as a case study, J. Exp. Bot. 66 (2015) 2913–2921, https://doi.org/10.1093/jxb/erv073.

[28] H. Yamasaki, Y. Sakihama, S. Takahashi, An alternative pathway for nitric oxide production in plants: new features of an old enzyme, Trends Plant Sci. 4 (1999) 128–129, https://doi.org/10.1016/S1360-1385(99)01393-X.

[29] F. Del Castello, A. Nejamkin, R. Cassia, N. Correa-Aragunde, B. Fernández, N. Foresi, C. Lombardo, L. Ramirez, L. Lamattina, The era of nitric oxide in plant biology: Twenty years tying up loose ends, Nitric Oxide 85 (2019) 17–27, https://doi.org/10.1016/j.niox.2019.01.013.

[30] P. Baldet, C. Devaux, C. Chevalier, R. Brouquisse, D. Just, P. Raymond, Contrasted responses to carbohydrate limitation in tomato fruit at two stages of

development, Plant Cell Environ. 25 (2002) 1639–1649, https://doi.org/10.1046/j.1365-3040.2002.00941.x.
[31] F.S. Farnese, P.E. Menezes-Silva, G.S. Gusman, J.A. Oliveira, When Bad Guys Become Good Ones: The Key Role of Reactive Oxygen Species and Nitric Oxide in the Plant Responses to Abiotic Stress, Front. Plant Sci. 7 (2016), https://doi.org/10.3389/fpls.2016.00471.
[32] S.-E. Lau, M.F. Hamdan, T.-L. Pua, N.B. Saidi, B.C. Tan, Plant Nitric Oxide Signaling under Drought Stress, Plants 10 (2021) 360, https://doi.org/10.3390/plants10020360.
[33] X. Wang, M. Ruan, Q. Wan, W. He, L. Yang, X. Liu, L. He, L. Yan, Y. Bi, Nitric oxide and hydrogen peroxide increase glucose-6-phosphate dehydrogenase activities and expression upon drought stress in soybean roots, Plant Cell Rep. 39 (2020) 63–73, https://doi.org/10.1007/s00299-019-02473-3.
[34] M. Khan, Q.M. Imran, M. Shahid, B.-G. Mun, S.-U. Lee, M.A. Khan, A. Hussain, I.-J. Lee, B.-W. Yun, Nitric oxide- induced AtAO3 differentially regulates plant defense and drought tolerance in Arabidopsis thaliana, BMC Plant Biol. 19 (2019) 602, https://doi.org/10.1186/s12870-019-2210-3.
[35] M. Caruso, A. Continella, G. Modica, C. Pannitteri, R. Russo, F. Salonia, C. Arlotta, A. Gentile, G. Russo, Rootstocks Influence Yield Precocity, Productivity, and Pre-Harvest Fruit Drop of Mandared Pigmented Mandarin, Agronomy 10 (2020) 1305, https://doi.org/10.3390/agronomy10091305.
[36] L. Aparicio-Durán, F.G. Gmitter Jr., J.M. Arjona-López, R. Calero-Velázquez, Á. Hervalejo, F.J. Arenas-Arenas, Water-stress influences on three new promising HLB-tolerant citrus rootstocks, Horticulturae 7 (2021) 336, https://doi.org/10.3390/horticulturae7100336.
[37] E. Scialò, A. Sicilia, A. Continella, A. Gentile, A.R. Lo Piero, Transcriptome profiling and weighted gene correlation network analysis reveal hub genes and pathways involved in the response to polyethylene-glycol-induced drought stress of two citrus rootstocks, Biology 13 (2024) 595, https://doi.org/10.3390/biology13080595.
[38] E. Scialò, A. Sicilia, A. Continella, G. Modica, A.R. Lo Piero, On the "priming" steps: initial results on the effect of PEG-induced drought stress upon the oxidative status and related gene expression in *Citrus* rootstocks, Acta Hortic. (2024) 131–138, https://doi.org/10.17660/ActaHortic.2024.1399.16.
[39] G. Tanou, C. Job, L. Rajjou, E. Arc, M. Belghazi, G. Diamantidis, A. Molassiotis, D. Job, Proteomics reveals the overlapping roles of hydrogen peroxide and nitric oxide in the acclimation of citrus plants to salinity, Plant J. 60 (2009) 795–804, https://doi.org/10.1111/j.1365-313X.2009.04000.x.
[40] D. Yavuz, M. Seymen, Ü. Kal, Z. Atakul, Ö.B. Tanrıverdi, Ö. Türkmen, N. Yavuz, Agronomic and physio-biochemical responses of lettuce to exogenous sodium nitroprusside (SNP) applied under different irrigation regimes, Agric. Water Manag. 277 (2023) 108127, https://doi.org/10.1016/j.agwat.2022.108127.
[41] E. Zangani, H.R. Angourani, B. Andalibi, S.V. Rad, A. Mastinu, Sodium Nitroprusside Improves the Growth and Behavior of the Stomata of Silybum marianum L. Subjected to Different Degrees of Drought, Life (Basel) 13 (2023) 875, https://doi.org/10.3390/life13040875.
[42] V. Ziogas, G. Tanou, M. Belghazi, P. Filippou, V. Fotopoulos, D. Grigorios, A. Molassiotis, Roles of sodium hydrosulfide and sodium nitroprusside as priming molecules during drought acclimation in citrus plants, Plant Mol. Biol. 89 (2015) 433–450, https://doi.org/10.1007/s11103-015-0379-x.
[43] C. López-Hidalgo, M. Meijón, L. Lamelas, L. Valledor, The rainbow protocol: A sequential method for quantifying pigments, sugars, free amino acids, phenolics, flavonoids and MDA from a small amount of sample, Plant Cell Environ. 44 (2021) 1977–1986, https://doi.org/10.1111/pce.14007.
[44] V. Velikova, I. Yordanov, A. Edreva, Oxidative stress and some antioxidant systems in acid rain-treated bean plants: Protective role of exogenous polyamines, Plant Sci. 151 (2000) 59–66, https://doi.org/10.1016/S0168-9452(99)00197-1.
[45] R. Core Team, 2024. R: A language and environment for statistical computing.
[46] Y. Benjamini, Y. Hochberg, Controlling the false discovery rate: a practical and powerful approach to multiple testing, J. R. Stat. Soc. Ser. B (Methodol.) 57 (1995) 289–300, https://doi.org/10.1111/j.2517-6161.1995.tb02031.x.
[47] S.X. Ge, D. Jung, R. Yao, ShinyGO: a graphical gene-set enrichment tool for animals and plants, Bioinformatics 36 (2020) 2628–2629, https://doi.org/10.1093/bioinformatics/btz931.
[48] D. Bu, H. Luo, P. Huo, Z. Wang, S. Zhang, Z. He, Y. Wu, L. Zhao, J. Liu, J. Guo, S. Fang, W. Cao, L. Yi, Y. Zhao, L. Kong, KOBAS-i: intelligent prioritization and exploratory visualization of biological functions for gene enrichment analysis, Nucleic Acids Res. 49 (2021) W317–W325, https://doi.org/10.1093/nar/gkab447.
[49] P. Langfelder, S. Horvath, WGCNA: an R package for weighted correlation network analysis, BMC Bioinforma. 9 (2008) 559, https://doi.org/10.1186/1471-2105-9-559.
[50] F. Takahashi, T. Kuromori, K. Urano, K. Yamaguchi-Shinozaki, K. Shinozaki, Drought Stress Responses and Resistance in Plants: From Cellular Responses to Long-Distance Intercellular Communication, Front. Plant Sci. 11 (2020), https://doi.org/10.3389/fpls.2020.556972.
[51] P. Salvi, M. Manna, H. Kaur, T. Thakur, N. Gandass, D. Bhatt, M. Muthamilarasan, Phytohormone signaling and crosstalk in regulating drought stress response in plants, Plant Cell Rep. 40 (2021) 1305–1329, https://doi.org/10.1007/s00299-021-02683-8.
[52] H. Guo, L. Li, H. Ye, X. Yu, A. Algreen, Y. Yin, Three related receptor-like kinases are required for optimal cell elongation in Arabidopsis thaliana, Proc. Natl. Acad. Sci. 106 (2009) 7648–7653, https://doi.org/10.1073/pnas.0812346106.
[53] K. Hématy, P.-E. Sado, A. Van Tuinen, S. Rochange, T. Desnos, S. Balzergue, S. Pelletier, J.-P. Renou, H. Höfte, A Receptor-like Kinase Mediates the Response of *Arabidopsis* Cells to the Inhibition of Cellulose Synthesis, Curr. Biol. 17 (2007) 922–931, https://doi.org/10.1016/j.cub.2007.05.018.
[54] D.F. Santoro, I. Puglisi, A. Sicilia, A. Baglieri, E. La Bella, A.R. Lo Piero, Transcriptomic profile of lettuce seedlings (Lactuca sativa) response to microalgae extracts used as biostimulant agents, AoB PLANTS 15 (2023) plad043, https://doi.org/10.1093/aobpla/plad043.
[55] T.A. Wagner, B.D. Kohorn, Wall-Associated Kinases Are Expressed throughout Plant Development and Are Required for Cell Expansion, Plant Cell 13 (2001) 303–318, https://doi.org/10.1105/tpc.13.2.303.
[56] Z. Liu, Y. Jia, Y. Ding, Y. Shi, Z. Li, Y. Guo, Z. Gong, S. Yang, Plasma Membrane CRPK1-Mediated Phosphorylation of 14-3-3 Proteins Induces Their Nuclear Import to Fine-Tune CBF Signaling during Cold Response, Mol. Cell 66 (2017) 117–128.e5, https://doi.org/10.1016/j.molcel.2017.02.016.
[57] R. Peyronnet, E.S. Haswell, H. Barbier-Brygoo, J.-M. Frachisse, AtMSL9 and AtMSL10: Sensors of plasma membrane tension in Arabidopsis roots, Plant Signal. Behav. 3 (2008) 726–729, https://doi.org/10.4161/psb.3.9.6487.
[58] F. Takahashi, T. Kuromori, K. Urano, K. Yamaguchi-Shinozaki, K. Shinozaki, Drought Stress Responses and Resistance in Plants: From Cellular Responses to Long-Distance Intercellular Communication, Front. Plant Sci. 11 (2020), https://doi.org/10.3389/fpls.2020.556972.
[59] K. Mori, N. Renhu, M. Naito, A. Nakamura, H. Shiba, T. Yamamoto, T. Suzaki, H. Iida, K. Miura, Ca2+-permeable mechanosensitive channels MCA1 and MCA2 mediate cold-induced cytosolic Ca2+ increase and cold tolerance in Arabidopsis, Sci. Rep. 8 (2018) 550, https://doi.org/10.1038/s41598-017-17483-y.
[60] F. Wu, Y. Chi, Z. Jiang, Y. Xu, L. Xie, F. Huang, D. Wan, J. Ni, F. Yuan, X. Wu, Y. Zhang, L. Wang, R. Ye, B. Byeon, W. Wang, S. Zhang, M. Sima, S. Chen, M. Zhu, J. Pei, D.M. Johnson, S. Zhu, X. Cao, C. Pei, Z. Zai, Y. Liu, T. Liu, G.B. Swift, W. Zhang, M. Yu, Z. Hu, J.N. Siedow, X. Chen, Z.-M. Pei, Hydrogen peroxide sensor HPCA1 is an LRR receptor kinase in Arabidopsis, Nature 578 (2020) 577–581, https://doi.org/10.1038/s41586-020-2032-3.
[61] M. Trujillo, K. Ichimura, C. Casais, K. Shirasu, Negative Regulation of PAMP-Triggered Immunity by an E3 Ubiquitin Ligase Triplet in Arabidopsis, Curr. Biol. 18 (2008) 1396–1401, https://doi.org/10.1016/j.cub.2008.07.085.
[62] S.K. Cho, M.Y. Ryu, C. Song, J.M. Kwak, W.T. Kim, Arabidopsis PUB22 and PUB23 Are Homologous U-Box E3 Ubiquitin Ligases That Play Combinatory Roles in Response to Drought Stress, Plant Cell 20 (2008) 1899–1914, https://doi.org/10.1105/tpc.108.060699.
[63] Y. Wang, J.H.G. Cordewener, A.H.P. America, W. Shan, K. Bouwmeester, F. Govers, Arabidopsis Lectin Receptor Kinases LecRK-IX.1 and LecRK-IX.2 Are Functional Analogs in Regulating Phytophthora Resistance and Plant Cell Death, MPMI 28 (2015) 1032–1048, https://doi.org/10.1094/MPMI-02-15-0025-R.
[64] H. Guo, J.R. Ecker, The ethylene signaling pathway: new insights, Curr. Opin. Plant Biol. 7 (2004) 40–49, https://doi.org/10.1016/j.pbi.2003.11.011.
[65] M. Ohto, S. Hayashi, S. Sawa, A. Hashimoto-Ohta, K. Nakamura, Involvement of HLS1 in Sugar and Auxin Signaling in Arabidopsis Leaves, Plant Cell Physiol. 47 (2006) 1603–1611, https://doi.org/10.1093/pcp/pcl027.
[66] R. Benjamins, A. Quint, D. Weijers, P. Hooykaas, R. Offringa, The PINOID protein kinase regulates organ development in Arabidopsis by enhancing polar auxin transport, Development 128 (2001) 4057–4067, https://doi.org/10.1242/dev.128.20.4057.
[67] M. Michniewicz, M.K. Zago, L. Abas, D. Weijers, A. Schweighofer, I. Meskiene, M. G. Heisler, C. Ohno, J. Zhang, F. Huang, R. Schwab, D. Weigel, E.M. Meyerowitz, C. Luschnig, R. Offringa, J. Friml, Antagonistic Regulation of PIN Phosphorylation by PP2A and PINOID Directs Auxin Flux, Cell 130 (2007) 1044–1056, https://doi.org/10.1016/j.cell.2007.07.033.
[68] J. Friml, X. Yang, M. Michniewicz, D. Weijers, A. Quint, O. Tietz, R. Benjamins, P. B.F. Ouwerkerk, K. Ljung, G. Sandberg, P.J.J. Hooykaas, K. Palme, R. Offringa, A PINOID-Dependent Binary Switch in Apical-Basal PIN Polar Targeting Directs Auxin Efflux, Science 306 (2004) 862–865, https://doi.org/10.1126/science.1100618.
[69] C.I. Cazzonelli, M. Vanstraelen, S. Simon, K. Yin, A. Carron-Arthur, N. Nisar, G. Tarle, A.J. Cuttriss, I.R. Searle, E. Benkova, U. Mathesius, J. Masle, J. Friml, B. J. Pogson, Role of the Arabidopsis PIN6 Auxin Transporter in Auxin Homeostasis and Auxin-Mediated Development, PLOS ONE 8 (2013) e70069, https://doi.org/10.1371/journal.pone.0070069.
[70] Y. Wang, L. Yang, Y. Tang, R. Tang, Y. Jing, Chi Zhang, B. Zhang, X. Li, Y. Cui, Chunhua Zhang, J. Shi, F. Zhao, W. Lan, S. Luan, Arabidopsis choline transporter-like 1 (CTL1) regulates secretory trafficking of auxin transporters to control seedling growth, PLOS Biol. 15 (2017) e2004310, https://doi.org/10.1371/journal.pbio.2004310.
[71] Y. Yang, R. Xu, C. Ma, A.C. Vlot, D.F. Klessig, E. Pichersky, Inactive Methyl Indole-3-Acetic Acid Ester Can Be Hydrolyzed and Activated by Several Esterases Belonging to the AtMES Esterase Family of Arabidopsis, Plant Physiol. 147 (2008) 1034–1045, https://doi.org/10.1104/pp.108.118224.
[72] B.C. Willige, S. Ahlers, M. Zourelidou, I.C.R. Barbosa, E. Demarsy, M. Trevisan, P. A. Davis, M.R.G. Roelfsema, R. Hangarter, C. Fankhauser, C. Schwechheimer, D6PK AGCVIII Kinases Are Required for Auxin Transport and Phototropic Hypocotyl Bending in Arabidopsis, Plant Cell 25 (2013) 1674–1688, https://doi.org/10.1105/tpc.113.111484.
[73] M. Zourelidou, I. Müller, B.C. Willige, C. Nill, Y. Jikumaru, H. Li, C. Schwechheimer, The polarly localized D6 PROTEIN KINASE is required for efficient auxin transport in Arabidopsis thaliana, Development 136 (2009) 627–636, https://doi.org/10.1242/dev.028365.
[74] N. Dai, W. Wang, S.E. Patterson, A.B. Bleecker, The TMK Subfamily of Receptor-Like Kinases in Arabidopsis Display an Essential Role in Growth and a Reduced

Sensitivity to Auxin, PLOS ONE 8 (2013) e60990, https://doi.org/10.1371/journal.pone.0060990.
[75] S. Kim, H. Choi, H.-J. Ryu, J.H. Park, M.D. Kim, S.Y. Kim, ARIA, an Arabidopsis Arm Repeat Protein Interacting with a Transcriptional Regulator of Abscisic Acid-Responsive Gene Expression, Is a Novel Abscisic Acid Signaling Component, Plant Physiol. 136 (2004) 3639–3648, https://doi.org/10.1104/pp.104.049189.
[76] Q. Bu, H. Li, Q. Zhao, H. Jiang, Q. Zhai, J. Zhang, X. Wu, J. Sun, Q. Xie, D. Wang, C. Li, The Arabidopsis RING Finger E3 Ligase RHA2a Is a Novel Positive Regulator of Abscisic Acid Signaling during Seed Germination and Early Seedling Development, Plant Physiol. 150 (2009) 463–481, https://doi.org/10.1104/pp.109.135269.
[77] H. Li, H. Jiang, Q. Bu, Q. Zhao, J. Sun, Q. Xie, C. Li, The Arabidopsis RING Finger E3 Ligase RHA2b Acts Additively with RHA2a in Regulating Abscisic Acid Signaling and Drought Response, Plant Physiol. 156 (2011) 550–563, https://doi.org/10.1104/pp.111.176214.
[78] A. Wawrzynska, K.M. Christiansen, Y. Lan, N.L. Rodibaugh, R.W. Innes, Powdery Mildew Resistance Conferred by Loss of the ENHANCED DISEASE RESISTANCE1 Protein Kinase Is Suppressed by a Missense Mutation in KEEP ON GOING, a Regulator of Abscisic Acid Signaling, Plant Physiol. 148 (2008) 1510–1522, https://doi.org/10.1104/pp.108.127605.
[79] M. Varbanova, S. Yamaguchi, Y. Yang, K. McKelvey, A. Hanada, R. Borochov, F. Yu, Y. Jikumaru, J. Ross, D. Cortes, C.J. Ma, J.P. Noel, L. Mander, V. Shulaev, Y. Kamiya, S. Rodermel, D. Weiss, E. Pichersky, Methylation of Gibberellins by Arabidopsis GAMT1 and GAMT2, Plant Cell 19 (2007) 32–45, https://doi.org/10.1105/tpc.106.044602.
[80] S. Lee, H. Cheng, K.E. King, W. Wang, Y. He, A. Hussain, J. Lo, N.P. Harberd, J. Peng, Gibberellin regulates Arabidopsis seed germination via RGL2, a GAI/RGA-like gene whose expression is up-regulated following imbibition, Genes Dev. 16 (2002) 646–658, https://doi.org/10.1101/gad.969002.
[81] O. Lorenzo, R. Piqueras, J.J. Sánchez-Serrano, R. Solano, ETHYLENE RESPONSE FACTOR1 Integrates Signals from Ethylene and Jasmonate Pathways in Plant Defense[W], Plant Cell 15 (2003) 165–178, https://doi.org/10.1105/tpc.007468.
[82] M. Berrocal-Lobo, A. Molina, Ethylene Response Factor 1 Mediates Arabidopsis Resistance to the Soilborne Fungus Fusarium oxysporum, MPMI 17 (2004) 763–770, https://doi.org/10.1094/MPMI.2004.17.7.763.
[83] M. Berrocal-Lobo, A. Molina, R. Solano, Constitutive expression of ETHYLENE-RESPONSE-FACTOR1 in Arabidopsis confers resistance to several necrotrophic fungi, Plant J. 29 (2002) 23–32, https://doi.org/10.1046/j.1365-313x.2002.01191.x.
[84] H. Sato, J. Mizoi, H. Tanaka, K. Maruyama, F. Qin, Y. Osakabe, K. Morimoto, T. Ohori, K. Kusakabe, M. Nagata, K. Shinozaki, K. Yamaguchi-Shinozaki, Arabidopsis DPB3-1, a DREB2A Interactor, Specifically Enhances Heat Stress-Induced Gene Expression by Forming a Heat Stress-Specific Transcriptional Complex with NF-Y Subunits, Plant Cell 26 (2014) 4954–4973, https://doi.org/10.1105/tpc.114.132928.
[85] G.R. Teakle, I.W. Manfield, J.F. Graham, P.M. Gilmartin, Arabidopsis thaliana GATA factors: organisation, expression and DNA-binding characteristics, Plant Mol. Biol. 50 (2002) 43–56, https://doi.org/10.1023/A:1016062325584.
[86] G. Benn, C.-Q. Wang, D.R. Hicks, J. Stein, C. Guthrie, K. Dehesh, A key general stress response motif is regulated non-uniformly by CAMTA transcription factors, Plant J. 80 (2014) 82–92, https://doi.org/10.1111/tpj.12620.
[87] H. Yu, X. Chen, Y.-Y. Hong, Y. Wang, P. Xu, S.-D. Ke, H.-Y. Liu, J.-K. Zhu, D. J. Oliver, C.-B. Xiang, Activated Expression of an Arabidopsis HD-START Protein Confers Drought Tolerance with Improved Root System and Reduced Stomatal Density, Plant Cell 20 (2008) 1134–1151, https://doi.org/10.1105/tpc.108.058263.
[88] K.K. Bhattarai, H.S. Atamian, I. Kaloshian, T. Eulgem, WRKY72-type transcription factors contribute to basal immunity in tomato and Arabidopsis as well as gene-for-gene resistance mediated by the tomato R gene Mi-1, Plant J. 63 (2010) 229–240, https://doi.org/10.1111/j.1365-313X.2010.04232.x.
[89] E.A. Spyropoulou, M.A. Haring, R.C. Schuurink, RNA sequencing on Solanum lycopersicum trichomes identifies transcription factors that activate terpene synthase promoters, BMC Genom. 15 (2014) 402, https://doi.org/10.1186/1471-2164-15-402.
[90] J. Zhou, R. Zhong, Z.-H. Ye, Arabidopsis NAC Domain Proteins, VND1 to VND5, Are Transcriptional Regulators of Secondary Wall Biosynthesis in Vessels, PLOS ONE 9 (2014) e105726, https://doi.org/10.1371/journal.pone.0105726.
[91] J.M. Romano, C. Dubos, M.B. Prouse, O. Wilkins, H. Hong, M. Poole, K.-Y. Kang, E. Li, C.J. Douglas, T.L. Western, S.D. Mansfield, M.M. Campbell, AtMYB61, an R2R3-MYB transcription factor, functions as a pleiotropic regulator via a small gene network, N. Phytol. 195 (2012) 774–786, https://doi.org/10.1111/j.1469-8137.2012.04201.x.
[92] Z. Xie, D. Li, L. Wang, F.D. Sack, E. Grotewold, Role of the stomatal development regulators FLP/MYB88 in abiotic stress responses, Plant J. 64 (2010) 731–739, https://doi.org/10.1111/j.1365-313X.2010.04364.x.
[93] Y. Oshima, N. Mitsuda, The MIXTA-like Transcription factor MYB16 is a major regulator of cuticle formation in vegetative organs, Plant Signal. Behav. 8 (2013) e26826, https://doi.org/10.4161/psb.26826.
[94] H.-S. Ma, D. Liang, P. Shuai, X.-L. Xia, W.-L. Yin, The salt- and drought-inducible poplar GRAS protein SCL7 confers salt and drought tolerance in Arabidopsis thaliana, J. Exp. Bot. 61 (2010) 4011–4019, https://doi.org/10.1093/jxb/erq217.
[95] S. Dhondt, F. Coppens, F. De Winter, K. Swarup, R.M.H. Merks, D. Inzé, M. J. Bennett, G.T.S. Beemster, SHORT-ROOT and SCARECROW Regulate Leaf Growth in Arabidopsis by Stimulating S-Phase Progression of the Cell Cycle, Plant Physiol. 154 (2010) 1183–1195, https://doi.org/10.1104/pp.110.158857.
[96] H. Cui, D. Kong, X. Liu, Y. Hao, SCARECROW, SCR-LIKE 23 and SHORT-ROOT control bundle sheath cell fate and function in rabidopsis thaliana, Plant J. 78 (2014) 319–327, https://doi.org/10.1111/tpj.12470.
[97] A. Żelisko, M. García-Lorenzo, G. Jackowski, S. Jansson, C. Funk, AtFtsH6 is involved in the degradation of the light-harvesting complex II during high-light acclimation and senescence, Proc. Natl. Acad. Sci. 102 (2005) 13699–13704, https://doi.org/10.1073/pnas.0503472102.
[98] H. Hu, A. Boisson-Dernier, M. Israelsson-Nordström, M. Böhmer, S. Xue, A. Ries, J. Godoski, J.M. Kuhn, J.I. Schroeder, Carbonic anhydrases are upstream regulators of CO2-controlled stomatal movements in guard cells, Nat. Cell Biol. 12 (2010) 87–93, https://doi.org/10.1038/ncb2009.
[99] K. Miwa, J. Takano, T. Fujiwara, Improvement of seed yields under boron-limiting conditions through overexpression of BOR1, a boron transporter for xylem loading, in Arabidopsis thaliana, Plant J. 46 (2006) 1084–1091, https://doi.org/10.1111/j.1365-313X.2006.02763.x.
[100] Y. Wang, Y. Liu, X. Pan, Y. Wan, Z. Li, Z. Xie, T. Hu, P. Yang, A 3-Ketoacyl-CoA Synthase 10 (KCS10) Homologue from Alfalfa Enhances Drought Tolerance by Regulating Cuticular Wax Biosynthesis, J. Agric. Food Chem. 71 (2023) 14493–14504, https://doi.org/10.1021/acs.jafc.3c03881.
[101] O. Bouchabke-Coussa, M.-L. Quashie, J. Seoane-Redondo, M.-N. Fortabat, C. Gery, A. Yu, D. Linderme, J. Trouverie, F. Granier, E. Téoulé, M. Durand-Tardif, ESKIMO1 is a key gene involved in water economy as well as cold acclimation and salt tolerance, BMC Plant Biol. 8 (2008) 125, https://doi.org/10.1186/1471-2229-8-125.
[102] V. Lefebvre, M.-N. Fortabat, A. Ducamp, H.M. North, A. Maia-Grondard, J. Trouverie, Y. Boursiac, G. Mouille, M. Durand-Tardif, ESKIMO1 Disruption in Arabidopsis Alters Vascular Tissue and Impairs Water Transport, PLOS ONE 6 (2011) e16645, https://doi.org/10.1371/journal.pone.0016645.
[103] R. Lugan, M.-F. Niogret, L. Kervazo, F.R. Larher, J. Kopka, A. Bouchereau, Metabolome and water status phenotyping of Arabidopsis under abiotic stress cues reveals new insight into ESK1 function, Plant Cell Environ. 32 (2009) 95–108, https://doi.org/10.1111/j.1365-3040.2008.01898.x.
[104] E. Pesquet, A.V. Korolev, G. Calder, C.W. Lloyd, The Microtubule-Associated Protein AtMAP70-5 Regulates Secondary Wall Patterning in *Arabidopsis* Wood Cells, Curr. Biol. 20 (2010) 744–749, https://doi.org/10.1016/j.cub.2010.02.057.
[105] T.S. Gechev, F. Van Breusegem, J.M. Stone, I. Denev, C. Laloi, Reactive oxygen species as signals that modulate plant stress responses and programmed cell death, BioEssays 28 (2006) 1091–1101, https://doi.org/10.1002/bies.20493.
[106] R. Mittler, ROS Are Good, Trends Plant Sci. 22 (2017) 11–19, https://doi.org/10.1016/j.tplants.2016.08.002.
[107] Á. Gallé, J. Csiszár, M. Secenji, A. Guóth, L. Cseuz, I. Tari, J. Györgyey, L. Erdei, Glutathione transferase activity and expression patterns during grain filling in flag leaves of wheat genotypes differing in drought tolerance: Response to water deficit, J. Plant Physiol. 166 (2009) 1878–1891, https://doi.org/10.1016/j.jplph.2009.05.016.
[108] G. Gullner, T. Komives, L. Király, P. Schröder, Glutathione S-Transferase Enzymes in Plant-Pathogen Interactions, Front. Plant Sci. 9 (2018), https://doi.org/10.3389/fpls.2018.01836.
[109] S. Islam, I.A. Rahman, T. Islam, A. Ghosh, Genome-wide identification and expression analysis of glutathione S-transferase gene family in tomato: Gaining an insight to their physiological and stress-specific roles, PLOS ONE 12 (2017) e0187504, https://doi.org/10.1371/journal.pone.0187504.
[110] A.R. Lo Piero, V. Mercurio, I. Puglisi, G. Petrone, Different roles of functional residues in the hydrophobic binding site of two sweet orange tau glutathione S-transferases, FEBS J. 277 (2010) 255–262, https://doi.org/10.1111/j.1742-4658.2009.07481.x.
[111] I. Nianiou-Obeidat, P. Madesis, C. Kissoudis, G. Voulgari, E. Chronopoulou, A. Tsaftaris, N.E. Labrou, Plant glutathione transferase-mediated stress tolerance: functions and biotechnological applications, Plant Cell Rep. 36 (2017) 791–805, https://doi.org/10.1007/s00299-017-2139-7.
[112] J.-X. Liu, H. Wang, K. Feng, T. Li, Y.-H. Liu, A.-Q. Duan, S. Shu, H. Liu, A.-S. Xiong, AgDHAR2, a chloroplast-located dehydroascorbate reductase, modulates the ascorbate accumulation and drought stress response in celery, Environ. Exp. Bot. 202 (2022) 105006, https://doi.org/10.1016/j.envexpbot.2022.105006.
[113] H.-H. Zhang, Nan Xu, Zhi-Yuan Teng, Jun-Rui Wang, Songliang Ma, Xuye Wu, Xin Li, G.-Y. Sun, 2-Cys Prx plays a critical role in scavenging H2O2 and protecting photosynthetic function in leaves of tobacco seedlings under drought stress, J. Plant Interact. 14 (2019) 119–128, https://doi.org/10.1080/17429145.2018.1562111.
[114] C. Zheng, X. Wang, Y. Xu, S. Wang, X. Jiang, X. Liu, W. Cui, Y. Wu, C. Yan, H. Liu, Y. Lu, J. Chen, J. Zhou, The peroxidase gene *OsPrx114* activated by OsWRKY50 enhances drought tolerance through ROS scavenging in rice, Plant Physiol. Biochem. 204 (2023) 108138, https://doi.org/10.1016/j.plaphy.2023.108138.
[115] A. Holmgren, THIOREDOXIN, Annu. Rev. Biochem. 54 (1985) 237–271, https://doi.org/10.1146/annurev.bi.54.070185.001321.
[116] J.-Y. Cha, J.Y. Kim, I.J. Jung, M.R. Kim, A. Melencion, S.S. Alam, D.-J. Yun, S. Y. Lee, M.G. Kim, W.-Y. Kim, NADPH-dependent thioredoxin reductase A (NTRA) confers elevated tolerance to oxidative stress and drought, Plant Physiol. Biochem. 80 (2014) 184–191, https://doi.org/10.1016/j.plaphy.2014.04.008.
[117] L.P. Gonçalves, R.L. Boscariol Camargo, M.A. Takita, M.A. Machado, W.S. dos Soares Filho, M.G.C. Costa, Rootstock-induced molecular responses associated with drought tolerance in sweet orange as revealed by RNA-Seq, BMC Genom. 20 (2019) 110, https://doi.org/10.1186/s12864-019-5481-z.

[118] B. Liang, S. Wan, Q. Ma, L. Yang, W. Hu, L. Kuang, J. Xie, D. Liu, Y. Liu, Transcriptome and Physiological Analyses of a Navel Orange Mutant with Improved Drought Tolerance and Water Use Efficiency Caused by Increases of Cuticular Wax Accumulation and ROS Scavenging Capacity, Int. J. Mol. Sci. 23 (2022) 5660, https://doi.org/10.3390/ijms23105660.
[119] C. Kaya, F. Uğurlar, C.S. Seth, Sodium nitroprusside modulates oxidative and nitrosative processes in Lycopersicum esculentum L. under drought stress, Plant Cell Rep. 43 (2024) 152, https://doi.org/10.1007/s00299-024-03238-3.
[120] M. Saeedi, H. Shirzad, P. Noruzi, G. Ghasemi, Foliar application of sodium nitroprusside alters the physicochemical properties, antioxidant capacities, and enzymatic activities of strawberry cv. Camarosa, Sci. Rep. 14 (2024) 1–11, https://doi.org/10.1038/s41598-024-81936-4.
[121] A. Kaur, Madhu, S.K. Upadhyay, Chapter 16 - Mechanosensitive ion channels in plants, in: S.K. Upadhyay (Ed.), Calcium Transport Elements in Plants, Academic Press, 2021, pp. 267–279, https://doi.org/10.1016/B978-0-12-821792-4.00005-9.
[122] Ishu, Shumayla, Madhu, S.K. Upadhyay, Complementation with *TaNCL2-A* reinstates growth and abiotic stress response in *atncl* mutant of Arabidopsis, Plant Sci. (2025) 353–112411, https://doi.org/10.1016/j.plantsci.2025.112411.
[123] P.J. Seo, J.-M. Park, S.K. Kang, S.-G. Kim, C.-M. Park, An Arabidopsis senescence-associated protein SAG29 regulates cell viability under high salinity, Planta 233 (2011) 189–200, https://doi.org/10.1007/s00425-010-1293-8.
[124] L. Xu, G. Xiang, Q. Sun, Y. Ni, Z. Jin, S. Gao, Y. Yao, Melatonin enhances salt tolerance by promoting MYB108A-mediated ethylene biosynthesis in grapevines, Hortic. Res. 6 (2019) 114, https://doi.org/10.1038/s41438-019-0197-4.
[125] V.S. Freitas, R. Miranda, S. de, J.H. Costa, D.F. Oliveira, S. de, Paula, O. de, E. Miguel, C. de, R.S. Freire, J.T. Prisco, E. Gomes-Filho, Ethylene triggers salt tolerance in maize genotypes by modulating polyamine catabolism enzymes associated with H2O2 production, Environ. Exp. Bot. 145 (2018) 75–86, https://doi.org/10.1016/j.envexpbot.2017.10.022.
[126] E. Gharbi, J.-P. Martínez, H. Benahmed, G. Lepoint, B. Vanpee, M. Quinet, S. Lutts, Inhibition of ethylene synthesis reduces salt-tolerance in tomato wild relative species *Solanum chilense*, J. Plant Physiol. 210 (2017) 24–37, https://doi.org/10.1016/j.jplph.2016.12.001.
[127] S.J. Wi, S.J. Jang, K.Y. Park, Inhibition of biphasic ethylene production enhances tolerance to abiotic stress by reducing the accumulation of reactive oxygen species in Nicotiana tabacum, Mol. Cells 30 (2010) 37–49, https://doi.org/10.1007/s10059-010-0086-z.
[128] G. Cebrián, J. Iglesias-Moya, A. García, J. Martínez, J. Romero, J.J. Regalado, C. Martínez, J.L. Valenzuela, M. Jamilena, Involvement of ethylene receptors in the salt tolerance response of Cucurbita pepo, Hortic. Res. 8 (2021) 73, https://doi.org/10.1038/s41438-021-00508-z.
[129] H. Dong, Z. Zhen, J. Peng, L. Chang, Q. Gong, N.N. Wang, Loss of ACS7 confers abiotic stress tolerance by modulating ABA sensitivity and accumulation in Arabidopsis, J. Exp. Bot. 62 (2011) 4875–4887, https://doi.org/10.1093/jxb/err143.
[130] T. Kuromori, M. Seo, K. Shinozaki, ABA Transport and Plant Water Stress Responses, Trends Plant Sci. 23 (2018) 513–522, https://doi.org/10.1016/j.tplants.2018.04.001.
[131] P. Achard, J.-P. Renou, R. Berthomé, N.P. Harberd, P. Genschik, Plant DELLAs Restrain Growth and Promote Survival of Adversity by Reducing the Levels of Reactive Oxygen Species, Curr. Biol. 18 (2008) 656–660, https://doi.org/10.1016/j.cub.2008.04.034.
[132] J.-H. Ko, S.H. Yang, A.H. Park, O. Lerouxel, K.-H. Han, ANAC012, a member of the plant-specific NAC transcription factor family, negatively regulates xylary fiber development in Arabidopsis thaliana, Plant J. 50 (2007) 1035–1048, https://doi.org/10.1111/j.1365-313X.2007.03109.x.
[133] Y.-K. Liang, C. Dubos, I.C. Dodd, G.H. Holroyd, A.M. Hetherington, M. M. Campbell, *At*MYB61, an R2R3-MYB Transcription Factor Controlling Stomatal Aperture in *Arabidopsis thaliana*, Curr. Biol. 15 (2005) 1201–1206, https://doi.org/10.1016/j.cub.2005.06.041.
[134] K. Das, A. Roychoudhury, Reactive oxygen species (ROS) and response of antioxidants as ROS-scavengers during environmental stress in plants, Front. Environ. Sci. 2 (2014), https://doi.org/10.3389/fenvs.2014.00053.
[135] Y. Sharma, Shumayla Ishu, S. Dixit, K. Singh, S.K. Upadhyay, Decoding the features and potential roles of respiratory burst oxidase homologs in bread wheat. Current, Plant Biol. 37 (2024) 100315, https://doi.org/10.1016/j.cpb.2023.100315.
[136] Y. Shi, Y.-L. Chang, H.-T. Wu, A. Shalmani, W.-T. Liu, W.-Q. Li, J.-W. Xu, K.-M. Chen, OsRbohB-mediated ROS production plays a crucial role in drought stress tolerance of rice, Plant Cell Rep. 39 (2020) 1767–1784, https://doi.org/10.1007/s00299-020-02603-2.
[137] C. Cheng, X. Xu, M. Gao, J. Li, C. Guo, J. Song, X. Wang, Genome-wide analysis of respiratory burst oxidase homologs in grape (Vitis vinifera L.), Int. J. Mol. Sci. 14 (2013) 24169–24186, https://doi.org/10.3390/ijms141224169.
[138] D.A. Drechsel, M. Patel, Respiration-dependent H2O2 removal in brain mitochondria via the thioredoxin/peroxiredoxin system *, J. Biol. Chem. 285 (2010) 27850–27858, https://doi.org/10.1074/jbc.M110.101196.
[139] E. Gelhaye, N. Rouhier, N. Navrot, J.P. Jacquot, The plant thioredoxin system, Cell. Mol. Life Sci. 62 (2005) 24–35, https://doi.org/10.1007/s00018-004-4296-4.